INTERNATIONAL JOURNAL OF
NUMERICAL ANALYSIS AND MODELING
Volume 15, Number 6, Pages 785–810

LOCAL ANALYSIS OF THE LOCAL DISCONTINUOUS GALERKIN METHOD WITH THE GENERALIZED ALTERNATING NUMERICAL FLUX FOR TWO-DIMENSIONAL SINGULARLY PERTURBED PROBLEM

YAO CHENG, QIANG ZHANG, AND HAIJIN WANG*

Abstract. In this paper, we analyze the local discontinuous Galerkin method with the generalized alternating numerical flux for two-dimensional singularly perturbed problem with outflow boundary layers. By virtue of the two-dimensional generalized Gauss-Radau projection and energy technique with suitable weight function, we obtain the double-optimal error estimate, namely, the convergence rate in L^2-norm out of the outflow boundary layer is optimal, and the width of boundary layer is quasi-optimal, when piecewise tensor product polynomial space on quasi-uniform Cartesian meshes are used. Numerical experiments are given to verify the theoretical results.

Key words. Local analysis, local discontinuous Galerkin method, generalized alternating numerical flux, error estimate, singularly perturbed problem.

1. Introduction

Let $\Omega = (0,1)^2$ be the unit square with boundary Γ, and $T > 0$ is a final time. Consider the following two-dimensional singularly perturbed (SP) problem

$$u_t - \varepsilon \triangle u + \boldsymbol{\beta} \cdot \nabla u + cu = f \quad \text{in} \quad \Omega \times (0, T], \tag{1a}$$

with the Dirichlet boundary condition

$$u(x, y, t) = g(x, y, t) \quad \text{on} \quad \Gamma \times (0, T], \tag{1b}$$

and the initial condition

$$u(x, y, 0) = u_0(x, y) \quad \text{in } \Omega. \tag{1c}$$

Here $0 < \varepsilon \ll 1$ is the diffusion coefficient, $\boldsymbol{\beta} = (\beta_1, \beta_2)$ is the convective velocity field. Without loss of generality, we assume β_1 and β_2 are positive constants. We also assume the given functions c, f, g and u_0 are smooth enough.

It is well known that the exact solution of the SP problem (1) may change rapidly in a narrow region nearby the outflow boundaries $x = 1$ and $y = 1$, and it always appear boundary layer with width $O(\varepsilon \log(1/\varepsilon))$. To give a nice numerical result to this problem, many algorithms have been presented and developed [17]. The local discontinuous Galerkin (LDG) method is a special class of DG methods which has received increasing interest during the last two decades. It was firstly introduced by Cockburn and Shu [8] for the convection-diffusion problems, motivated by the successful numerical experiment of Bassi and Rebay [1] for compressible Navier-Stokes problems. Since the discontinuous finite element spaces do not require any continuity at interface boundaries, the LDG method is very good at solving those fast-varying, even those discontinuous solutions [11]. For more knowledge about this method, please refer to the review paper [21] and the reference therein.

Received by the editors November 25, 2017 and, in revised form, January 30, 2018.
2000 *Mathematics Subject Classification.* 65M12, 65M15, 65M60.
*Corresponding author.

There have been many global error analysis of the LDG methods for convection diffusion problems, for example [3, 9, 15, 19, 21], where the exact solution is assumed to be smooth enough in the whole domain. However, for SP problems, the exact solutions often have no uniform smoothness in the whole domain, and the corresponding global results become useless. To show the numerical advantage of the LDG method for SP problems, local analysis has been carried out in [5, 6, 23], where the *double-optimal* local error estimate was obtained. Here *double-optimal* means that the convergence rate in L^2-norm out of the outflow boundary layer is optimal, and the width of boundary layer is quasi-optimal. Numerical methods related to this topic also include the space-time DG method [13], the interior penalty DG method [10], continuous interior penalty method [2] and so on.

It is worthy to point out that, in [5, 6, 23] the double-optimal error estimates were established for purely alternating numerical flux, which means the purely upwind numerical flux for the convection and the purely alternating fluxes for the diffusion. However, this type of flux is often not easy to define for linear equations with varying-coefficients or even nonlinear equations [4]. From the view of practice, the generalized alternating numerical flux (GANF) is used more widely in the LDG method. Recently, motivated by the optimal error estimate of an upwind-biased DG method [16], we studied the LDG method with GANF for linear convection-diffusion problems in [4]. By virtue of the generalized Gauss-Radau (GGR) projection [15, 16], we obtained the optimal L^2-norm error estimate in the whole domain. Furthermore, by establishing the sharp approximation property of the one-dimensional GGR (1-d GGR) projection with the weight function, we also derived in [7] the double-optimal local error estimate for the one-dimensional SP problem with stationary outflow boundary layer.

The objective of this paper is to extend the results of [7] to the two-dimensional SP problems with stationary outflow boundary layers. We will present the local stability and show the double-optimal local error estimate of LDG method with GANF for $\mathcal{Q}^k$ element on quasi-uniform Cartesian meshes, where $\mathcal{Q}^k$ means the space of polynomials of degree at most $k \geq 0$ in each variable.

As an important ingredient in the local analysis, the weight function must be defined carefully. In this paper, we take it as the exponential decay function along each spatial directions. Besides, to achieve the double optimal local error estimate, our main technique is the two-dimensional GGR (2-d GGR) projection. The corresponding properties of 2-d GGR projections with the weight function are not easy to be established. Specifically, there are mainly two issues we have to consider.

(1) One is to obtain the optimal approximation property of 2-d GGR projections with weight function. Since the 2-d GGR projections have much complex expressions under the Dirichlet boundary condition, the direct manipulations based on the matrix analysis as [7] is much involved. The main difficulty is caused by the definition of GGR projection at the corner points. To overcome this difficulty, we will carefully investigate the structures of coefficient matrices and use some properties of tensor product of matrices.
(2) The other is to get the superconvergence property of 2-d GGR projections with weight function. Different from one dimensional case, the approximation errors for 2-d GGR projections can not be completely eliminated, in each element and on the interior element boundaries. To derive the optimal error estimate, we need to explore the superconvergence property, which has been discussed in [4], where the 2-d GGR projection under periodic boundary condition was considered. However, in the local error

analysis, this property equipped with suitable weight function need to be established.

The rest of this paper is organized as follows. In Section 2, we present the LDG scheme based on GANF for the two-dimensional SP problem. In Section 3, we present the local stability analysis by virtue of the local L^2 projection and the suitable weight function. Section 4 is the main body of this paper, where the double-optimal local error estimate are established with the help of the 2-d GGR projection. In Section 5, we present some numerical experiments to verify the theoretical results. Some concluding remarks and some technical proofs are given in Section 6 and Appendix, respectively.

2. LDG scheme

Let $\Omega_h = \{K_{ij}\}_{i=1,\dots,N_x}^{j=1,\dots,N_y}$ be a quasi-uniform rectangular tessellation of Ω with element $K_{ij} = I_i \times J_j$, where $I_i = (x_{i-\frac{1}{2}}, x_{i+\frac{1}{2}})$ and $J_j = (y_{j-\frac{1}{2}}, y_{j+\frac{1}{2}})$. Denote by the maximum cell size $h = \max\limits_{K\in\Omega_h} h_K$, where h_K is the diameter of element K. The associated finite element space is defined as

$$V_h \equiv \{v \in L^2(\Omega) : v|_K \in \mathcal{Q}^k(K), \forall K \in \Omega_h\}, \tag{2}$$

where $\mathcal{Q}^k(K)$ denotes the space of polynomials of degree at most $k \geq 0$ in each variable on K. Obviously, this space is contained in the following broken Sobolev space

$$H^m(\Omega_h) \equiv \{v \in L^2(\Omega) : v|_K \in H^m(K), \forall K \in \Omega_h\}, \quad m \geq 1, \tag{3}$$

whose function is allowed to have discontinuities across the element interfaces. Denote $v^{\pm}_{i+\frac{1}{2},y} = \lim_{x\to x^{\pm}_{i+\frac{1}{2}}} v(x,y)$ and $v^{\pm}_{x,j+\frac{1}{2}} = \lim_{y\to y^{\pm}_{j+\frac{1}{2}}} v(x,y)$ by the traces along different directions. We define the jumps and the weighted averages as

$$[\![v]\!]_{i+\frac{1}{2},y} = v^{+}_{i+\frac{1}{2},y} - v^{-}_{i+\frac{1}{2},y}, \qquad [\![v]\!]_{x,j+\frac{1}{2}} = v^{+}_{x,j+\frac{1}{2}} - v^{-}_{x,j+\frac{1}{2}}, \tag{4a}$$

$$v^{\alpha,y}_{i+\frac{1}{2},y} = \alpha v^{-}_{i+\frac{1}{2},y} + \widetilde{\alpha} v^{+}_{i+\frac{1}{2},y}, \qquad v^{x,\alpha}_{x,j+\frac{1}{2}} = \alpha v^{-}_{x,j+\frac{1}{2}} + \widetilde{\alpha} v^{+}_{x,j+\frac{1}{2}}, \tag{4b}$$

for any $i = 1, 2, \cdots, N_x - 1$ and $j = 1, 2, \cdots, N_y - 1$. Definition (4b) can be also extended to $i = 0, N_x$ and $j = 0, N_y$ with some special parameters, which will be given in the later analysis. Here and below, we use the simplified notation $\widetilde{\alpha} = 1-\alpha$ for an arbitrary parameter α.

By introducing two auxiliary variables $p = \sqrt{\varepsilon} u_x$ and $q = \sqrt{\varepsilon} u_y$, equation (1) can be written in the following equivalent first-order system

$$u_t + (\beta_1 u - \sqrt{\varepsilon} p)_x + (\beta_2 u - \sqrt{\varepsilon} q)_y + cu = f, \tag{5a}$$

$$p = \sqrt{\varepsilon} u_x, \tag{5b}$$

$$q = \sqrt{\varepsilon} u_y. \tag{5c}$$

The LDG scheme is to seek $u_h, p_h, q_h \in V_h$, such that in each element $K_{ij} \in \Omega_h$, the following variational forms

$$\begin{aligned}\int_{K_{ij}} \Big[\big((u_h)_t + cu_h\big)v_h - \big(\beta_1 u_h - \sqrt{\varepsilon}p_h\big)(v_h)_x - \big(\beta_2 u_h - \sqrt{\varepsilon}q_h\big)(v_h)_y\Big]\mathrm{d}x\mathrm{d}y \\ + \int_{J_j} \Big[(\hat{h}_{1u}v_h^-)_{i+\frac{1}{2},y} - (\hat{h}_{1u}v_h^+)_{i-\frac{1}{2},y}\Big]\mathrm{d}y \\ + \int_{I_i} \Big[(\hat{h}_{2u}v_h^-)_{x,j+\frac{1}{2}} - (\hat{h}_{2u}v_h^+)_{x,j-\frac{1}{2}}\Big]\mathrm{d}x = \int_{K_{ij}} f v_h \mathrm{d}x\mathrm{d}y,\end{aligned} \tag{6a}$$

$$\int_{K_{ij}} \Big[p_h r_h + \sqrt{\varepsilon}u_h(r_h)_x\Big]\mathrm{d}x\mathrm{d}y + \int_{J_j} \Big[(\hat{h}_p r_h^-)_{i+\frac{1}{2},y} - (\hat{h}_p r_h^+)_{i-\frac{1}{2},y}\Big]\mathrm{d}y = 0, \tag{6b}$$

$$\int_{K_{ij}} \Big[q_h s_h + \sqrt{\varepsilon}u_h(s_h)_y\Big]\mathrm{d}x\mathrm{d}y + \int_{I_i} \Big[(\hat{h}_q s_h^-)_{x,j+\frac{1}{2}} - (\hat{h}_q s_h^+)_{x,j-\frac{1}{2}}\Big]\mathrm{d}x = 0, \tag{6c}$$

hold for all test functions $v_h, r_h, s_h \in V_h$. The "hat" terms in (6) are the so-called numerical fluxes which are very important in the design of LDG methods. In this paper, we would like to adopt the generalized alternating numerical flux, similar as [4]. Namely, on the interior element interfaces, we define

$$(\hat{h}_{1u}, \hat{h}_p)_{i+\frac{1}{2},y} = (\beta_1 u_h^{\theta_1,y} - \sqrt{\varepsilon}p_h^{\widetilde{\theta_1},y}, -\sqrt{\varepsilon}u_h^{\theta_1,y})_{i+\frac{1}{2},y}, \quad i = 1, \ldots, N_x - 1, \tag{7a}$$

$$(\hat{h}_{2u}, \hat{h}_q)_{x,j+\frac{1}{2}} = (\beta_2 u_h^{x,\theta_2} - \sqrt{\varepsilon}q_h^{x,\widetilde{\theta_2}}, -\sqrt{\varepsilon}u_h^{x,\theta_2})_{x,j+\frac{1}{2}}, \quad j = 1, \ldots, N_y - 1, \tag{7b}$$

with $\theta_1 > \frac{1}{2}$ and $\theta_2 > \frac{1}{2}$. Obviously, they are purely alternating numerical flux when $\theta_1 = \theta_2 = 1$. If the element boundary lies on Γ, we define the numerical fluxes similarly as [3, 5–7], i.e.

$$(\hat{h}_{1u}, \hat{h}_p)_{\frac{1}{2},y} = (\beta_1 g - \sqrt{\varepsilon}p_h^+, -\sqrt{\varepsilon}g)_{\frac{1}{2},y}, \tag{7c}$$

$$(\hat{h}_{2u}, \hat{h}_q)_{x,\frac{1}{2}} = (\beta_2 g - \sqrt{\varepsilon}q_h^+, -\sqrt{\varepsilon}g)_{x,\frac{1}{2}}, \tag{7d}$$

and

$$(\hat{h}_{1u}, \hat{h}_p)_{N_x+\frac{1}{2},y} = (\beta_1 u_h^- - \gamma_1(g - u_h^-) - \sqrt{\varepsilon}p_h^-, -\sqrt{\varepsilon}g)_{N_x+\frac{1}{2},y}, \tag{7e}$$

$$(\hat{h}_{2u}, \hat{h}_q)_{x,N_y+\frac{1}{2}} = (\beta_2 u_h^- - \gamma_2(g - u_h^-) - \sqrt{\varepsilon}q_h^-, -\sqrt{\varepsilon}g)_{x,N_y+\frac{1}{2}}. \tag{7f}$$

Here γ_1 and γ_2 depend on the ratio of viscosity coefficient and mesh size, in this paper we take $\gamma_1 = \gamma_2 = \varepsilon/h$.

The initial solution can be taken as any $(k+1)$-th order approximation of u_0, for example, $u_h(0) = \Pi_h u_0$, where Π_h is the standard local L^2-projection onto V_h. Namely, for any function $z \in L^2(\Omega)$, the projection $\Pi_h z$ is defined as the unique function in V_h such that in each $K \in \Omega_h$, there holds

$$\langle \Pi_h z - z, v_h \rangle_K = 0, \quad \forall v_h \in \mathcal{Q}^k(K), \tag{8}$$

where $\langle \cdot, \cdot \rangle_K$ is the standard inner product in $L^2(K)$.

Till now we have completed the definition of the LDG scheme for problem (1). To facilitate the analysis, we sum up the variation forms in (6) over all elements and obtain the following compact form: find $\boldsymbol{w}_h = (u_h, p_h, q_h) \in \boldsymbol{V_h} \equiv (V_h)^3$, such that

$$\langle (u_h)_t, v_h \rangle + B_h(\boldsymbol{w}_h, \boldsymbol{\chi}_h) = F_h(t; \boldsymbol{\chi}_h), \quad \forall \boldsymbol{\chi}_h = (v_h, r_h, s_h) \in \boldsymbol{V_h}, \tag{9}$$

where $\langle\cdot,\cdot\rangle = \sum_K \langle\cdot,\cdot\rangle_K$. The bilinear functional in (9) is defined by

$$\begin{aligned}
B_h(\boldsymbol{w}_h,\boldsymbol{\chi}_h) &= \langle cu_h, v_h\rangle + \langle p_h, r_h\rangle + \langle q_h, s_h\rangle - \mathcal{H}_1(u_h,v_h) - \mathcal{H}_2(u_h,v_h)\\
&\quad + \sqrt{\varepsilon}\big[\mathcal{K}_1^{\theta_1}(u_h,r_h) + \mathcal{K}_2^{\theta_2}(u_h,s_h)\big] + \sqrt{\varepsilon}\big[\mathcal{L}_1^{\widetilde{\theta}_1}(p_h,v_h) + \mathcal{L}_2^{\widetilde{\theta}_2}(q_h,v_h)\big],
\end{aligned} \tag{10}$$

with

$$\begin{aligned}
\mathcal{H}_1(w,v) &= \langle \beta_1 w, v_x\rangle\\
&\quad + \sum_{j=1}^{N_y}\int_{J_j}\Big(\sum_{i=1}^{N_x-1}\beta_1(w^{\theta_1,y}[\![v]\!])_{i+\frac12,y} - (\beta_1+\gamma_1)(wv)^-_{N_x+\frac12,y}\Big)\mathrm{d}y,\\
\mathcal{H}_2(w,v) &= \langle \beta_2 w, v_y\rangle\\
&\quad + \sum_{i=1}^{N_x}\int_{I_i}\Big(\sum_{j=1}^{N_y-1}\beta_2(w^{x,\theta_2}[\![v]\!])_{x,j+\frac12} - (\beta_2+\gamma_2)(wv)^-_{x,N_y+\frac12}\Big)\mathrm{d}x,\\
\mathcal{K}_1^{\theta_1}(w,v) &= \langle w, v_x\rangle + \sum_{j=1}^{N_y}\int_{J_j}\sum_{i=1}^{N_x-1}(w^{\theta_1,y}[\![v]\!])_{i+\frac12,y}\mathrm{d}y,\\
\mathcal{K}_2^{\theta_2}(w,v) &= \langle w, v_y\rangle + \sum_{i=1}^{N_x}\int_{I_i}\sum_{j=1}^{N_y-1}(w^{x,\theta_2}[\![v]\!])_{x,j+\frac12}\mathrm{d}x,\\
\mathcal{L}_1^{\widetilde{\theta}_1}(w,v) &= \langle w, v_x\rangle + \sum_{j=1}^{N_y}\int_{J_j}\Big(\sum_{i=1}^{N_x-1}(w^{\widetilde{\theta}_1,y}[\![v]\!])_{i+\frac12,y} - (wv)^-_{N_x+\frac12,y} + (wv)^+_{\frac12,y}\Big)\mathrm{d}y,\\
\mathcal{L}_2^{\widetilde{\theta}_2}(w,v) &= \langle w, v_y\rangle + \sum_{i=1}^{N_x}\int_{I_i}\Big(\sum_{j=1}^{N_y-1}(w^{x,\widetilde{\theta}_2}[\![v]\!])_{x,j+\frac12} - (wv)^-_{x,N_y+\frac12} + (wv)^+_{x,\frac12}\Big)\mathrm{d}x,
\end{aligned}$$

for any $w, v \in H^1(\Omega_h)$. The linear functional in (9) is defined by

$$\begin{aligned}
F_h(t;\boldsymbol{\chi}_h) = \langle f, v_h\rangle &+ \sum_{j=1}^{N_y}\int_{J_j}\big[\gamma_1(gv_h^-)_{N_x+\frac12,y} + \beta_1(gv_h^+)_{\frac12,y}\big]\mathrm{d}y\\
&+ \sum_{i=1}^{N_x}\int_{I_i}\big[\gamma_2(gv_h^-)_{x,N_y+\frac12} + \beta_2(gv_h^+)_{x,\frac12}\big]\mathrm{d}x\\
&+ \sqrt{\varepsilon}\sum_{j=1}^{N_y}\int_{J_j}\big[(gr_h^-)_{N_x+\frac12,y} - (gr_h^+)_{\frac12,y}\big]\mathrm{d}y\\
&+ \sqrt{\varepsilon}\sum_{i=1}^{N_x}\int_{I_i}\big[(gs_h^-)_{x,N_y+\frac12} - (gs_h^+)_{x,\frac12}\big]\mathrm{d}x.
\end{aligned} \tag{11}$$

There hold the following relationships which will be used frequently in this paper.

Lemma 2.1. *For any $w, v \in H^1(\Omega_h)$, there hold identities*

$$\mathcal{L}_1^{\widetilde{\theta}_1}(w,v) = -\mathcal{K}_1^{\theta_1}(v,w), \quad \mathcal{L}_2^{\widetilde{\theta}_2}(w,v) = -\mathcal{K}_2^{\theta_2}(v,w). \tag{12}$$

Proof. They are obtained directly by using integration by parts and some trivial manipulations, so we omit the details here. □

3. Local stability

In this section we devote us to obtaining the local stability for the considered LDG scheme. We will first give some notations, then introduce the weight function as well as some related properties. After that, we present two important properties of LDG spatial discretization, and the local stability result.

3.1. Some notations. Denote $\|\cdot\|_{L^2(D)}$ as the standard L^2 norm in D, and drop the subscript if $D=\Omega$. For any $z\in H^1(\Omega_h)$, define

$$\|z\|_{\Gamma_h}=\Bigg\{\sum_{j=1}^{N_y}\int_{J_j}\sum_{i=1}^{N_x}\Big[(z^-_{i+\frac12,y})^2+(z^+_{i-\frac12,y})^2\Big]\mathrm{d}y + \sum_{i=1}^{N_x}\int_{I_i}\sum_{j=1}^{N_y}\Big[(z^-_{x,j+\frac12})^2+(z^+_{x,j-\frac12})^2\Big]\mathrm{d}x\Bigg\}^{\frac12}, \tag{13}$$

as the L^2 norm of function z on all element interfaces Γ_h. Furthermore, for any $z\in H^m(D_h)$ with $m\geq 0$ and a collection of elements set D_h, assume that ψ is an arbitrary weight function, we define the weighted semi-norm as

$$|z|_{\psi,m,D_h}=\Bigg\{\sum_{i+j=m}\sum_{K\in D_h}\int_K(\psi D_x^iD_y^jz)^2\mathrm{d}x\mathrm{d}y\Bigg\}^{\frac12}, \tag{14}$$

where D_x^iz denotes the i-th order derivative of z with respect to the spatial variable x (similar comments can be applied to D_y^jz). If $\psi=1$ or $D_h=\Omega_h$, we will omit the corresponding subscripts.

3.2. Weight function and related properties. In this paper, we employ the weight function

$$\psi(x,y)=\varphi\Big(\frac{x-x_0}{\sigma h}\Big)\varphi\Big(\frac{y-y_0}{\sigma h}\Big) \tag{15}$$

with cut-off function

$$\varphi(r)=\begin{cases}e^{-r}, & r>0,\\ 2-e^{r}, & r\leq 0,\end{cases} \tag{16}$$

where $\sigma\geq 2$ is a sufficiently large constant and $(x_0,y_0)\in\Omega$ is a fixed point which will be given in the local analysis. The similar weight functions have been adopted in [5–7, 13, 22]. This weight function satisfies the following elemental properties [5–7]:

(1) It is bounded. Namely, $\psi(x,y)\in(1,4)$ if $(x,y)\in\Omega_0\equiv(0,x_0)\times(0,y_0)$, and $\psi(x,y)\in(0,2h^\mu)$ if $x\geq x_0+\mu\sigma h\log\frac1h$ or $y\geq y_0+\mu\sigma h\log\frac1h$ with any $\mu>0$.

(2) It is decreasing in both x and y direction. Namely, $\psi_x<0$ and $\psi_y<0$.

(3) Its derivatives have similar form in the sense

$$|\psi_x|\leq C(\sigma h)^{-1}|\psi|,\quad |\psi_y|\leq C(\sigma h)^{-1}|\psi|. \tag{17}$$

Here and below, the symbol C denotes a generic positive constant independent of σ,x_0,y_0,h and ε. It may have different value at each occurrence.

(4) On any domain D of diameter σh,

$$RO(D,\psi)+RO(D,\psi_x)+RO(D,\psi_y)\leq C, \tag{18}$$

where $RO(D,v) = \max_{(x,y)\in D} |v(x,y)| / \min_{(x,y)\in D} |v(x,y)|$ represents the relative oscillation [14] on domain D. This property implies that the weight function is smooth and changes slowly in a local region.

Based on the properties (17) and (18), we can set up the following inverse inequalities and approximation properties. Similar discussion for these conclusions can be found in [5–7], so we omit the detailed proofs here.

Lemma 3.1. *For any $z_h \in V_h$, there hold*

$$|z_h|_{\psi,1} \le Ch^{-1}\|\psi z_h\|, \quad \|\psi z_h\|_{\Gamma_h} \le Ch^{-\frac{1}{2}}\|\psi z_h\|. \tag{19}$$

Lemma 3.2. *Let z be a given function, and denote by $\Pi_h^{\perp} z = z - \Pi_h z$ the L^2-projection error. There holds the following approximation properties:*

(1) *If $z \in H^{s+1}(\Omega_h)$ with $s \ge 0$, then*

$$\|\psi \Pi_h^{\perp} z\| + h^{\frac{1}{2}}\|\psi \Pi_h^{\perp} z\|_{\Gamma_h} \le Ch^{\min(k,s)+1}|z|_{\psi,s+1}. \tag{20}$$

(2) *If $z_h \in V_h$, then*

$$\|\psi^{-1}\Pi_h^{\perp}(\psi^2 z_h)\| + h^{\frac{1}{2}}\|\psi^{-1}\Pi_h^{\perp}(\psi^2 z_h)\|_{\Gamma_h} \le Ch^{\frac{1}{2}}\sigma^{-\frac{1}{2}}\||\psi\nabla\psi|^{\frac{1}{2}} z_h\| \tag{21a}$$

$$\le C\sigma^{-1}\|\psi z_h\|, \tag{21b}$$

where $\psi^{-1} = 1/\psi$.

Remark that the super-approximation property (21) will play an important role in the local stability analysis.

3.3. Properties of LDG spatial discretization. In this subsection, we derive two properties for the LDG spatial discretization under the following weighted norm

$$\begin{aligned}\|\boldsymbol{\chi}\|_\star \equiv \Big[&\|\psi v\|^2 + \|\psi r\|^2 + \|\psi s\|^2 + \beta_1\||\psi\psi_x|^{\frac{1}{2}} v\|^2 + \mathbb{J}_{x,\theta_1}^2(\psi v) \\ &+ \beta_2\||\psi\psi_y|^{\frac{1}{2}} v\|^2 + \mathbb{J}_{y,\theta_2}^2(\psi v)\Big]^{\frac{1}{2}},\end{aligned} \tag{22}$$

for any function $\boldsymbol{\chi} = (v,r,s) \in \boldsymbol{H^1}(\Omega_h) \equiv (H^1(\Omega_h))^3$, where

$$\mathbb{J}_{x,\theta_1}(v) = \left\{\sum_{j=1}^{N_y}\int_{J_j}\Big(\frac{1}{2}\beta_1(v^+)^2_{\frac{1}{2},y} + \sum_{i=1}^{N_x-1}\beta_1(\theta_1-\frac{1}{2})[\![v]\!]^2_{i+\frac{1}{2},y} + (\frac{1}{2}\beta_1+\gamma_1)(v^-)^2_{N_x+\frac{1}{2},y}\Big)\mathrm{d}y\right\}^{\frac{1}{2}},$$

$$\mathbb{J}_{y,\theta_2}(v) = \left\{\sum_{i=1}^{N_x}\int_{I_i}\Big(\frac{1}{2}\beta_2(v^+)^2_{x,\frac{1}{2}} + \sum_{j=1}^{N_y-1}\beta_2(\theta_2-\frac{1}{2})[\![v]\!]^2_{x,j+\frac{1}{2}} + (\frac{1}{2}\beta_2+\gamma_2)(v^-)^2_{x,N_y+\frac{1}{2}}\Big)\mathrm{d}x\right\}^{\frac{1}{2}},$$

are related to the definition of numerical fluxes.

Lemma 3.3. *Suppose $\varepsilon < h$. For any function $\boldsymbol{\chi} = (v,r,s) \in \boldsymbol{H^1}(\Omega_h)$, there holds*

$$B_h(\boldsymbol{\chi}, \psi^2\boldsymbol{\chi}) \ge (1 - C\sigma^{-\frac{1}{2}})\|\boldsymbol{\chi}\|_\star^2 - C\|\psi v\|^2, \tag{24}$$

where the bounding constant $C > 0$ is independent of $\sigma, h, x_0, y_0, \boldsymbol{\chi}$ and ε.

Proof. It is followed from (10) that

$$B_h(\boldsymbol{\chi}, \psi^2\boldsymbol{\chi}) = \left\langle cv, \psi^2 v\right\rangle + \|\psi r\|^2 + \|\psi s\|^2 + \Upsilon_1 + \Upsilon_2 + \Upsilon_3, \tag{25}$$

where

$$\Upsilon_1 = -\mathcal{H}_1(v, \psi^2 v) - \mathcal{H}_2(v, \psi^2 v), \tag{26a}$$

$$\Upsilon_2 = \sqrt{\varepsilon}\mathcal{K}_1^{\theta_1}(v, \psi^2 r) + \sqrt{\varepsilon}\mathcal{L}_1^{\widetilde{\theta_1}}(r, \psi^2 v), \tag{26b}$$

$$\Upsilon_3 = \sqrt{\varepsilon}\mathcal{K}_2^{\theta_2}(v, \psi^2 s) + \sqrt{\varepsilon}\mathcal{L}_2^{\widetilde{\theta_2}}(s, \psi^2 v), \tag{26c}$$

which will be estimated separately.

After a trivial manipulation and integration by parts, we get that

$$\begin{aligned}\left\langle v, (\psi^2 v)_x\right\rangle &= \langle v, \psi\psi_x v\rangle + \left\langle 1, (\frac{1}{2}\psi^2 v^2)_x\right\rangle \\ &= \langle v, \psi\psi_x v\rangle - \sum_{j=1}^{N_y}\int_{J_j}\Big[\frac{1}{2}(\psi v^+)^2_{\frac{1}{2},y} + \sum_{i=1}^{N_x-1}\frac{1}{2}[\![\psi^2 v^2]\!]_{i+\frac{1}{2},y} - \frac{1}{2}(\psi v^-)^2_{N_x+\frac{1}{2},y}\Big]\mathrm{d}y.\end{aligned}$$

Observing that

$$v^{\theta_1,y}_{i+\frac{1}{2},y}[\![\psi^2 v]\!]_{i+\frac{1}{2},y} - \frac{1}{2}[\![\psi^2 v^2]\!]_{i+\frac{1}{2},y} = -(\theta_1 - \frac{1}{2})[\![\psi v]\!]^2_{i+\frac{1}{2},y}$$

for any $i = 1, 2, \cdots, N_x - 1$, and the fact that $\psi_x < 0$, we obtain

$$\mathcal{H}_1(v, \psi^2 v) = -\beta_1\||\psi\psi_x|^{\frac{1}{2}}v\|^2 - \mathbb{J}^2_{x,\theta_1}(\psi v).$$

Similarly, $\mathcal{H}_2(v, \psi^2 v) = -\beta_2\||\psi\psi_y|^{\frac{1}{2}}v\|^2 - \mathbb{J}^2_{y,\theta_2}(\psi v)$. Thus we obtain

$$\Upsilon_1 = \beta_1\||\psi\psi_x|^{\frac{1}{2}}v\|^2 + \beta_2\||\psi\psi_y|^{\frac{1}{2}}v\|^2 + \mathbb{J}^2_{x,\theta_1}(\psi v) + \mathbb{J}^2_{y,\theta_2}(\psi v). \tag{27}$$

By Lemma 2.1 and a direct manipulation, we have

$$|\Upsilon_2| = \left|\sqrt{\varepsilon}\mathcal{K}_1^{\theta_1}(v, \psi^2 r) - \sqrt{\varepsilon}\mathcal{K}_1^{\theta_1}(\psi^2 v, r)\right| = |2\sqrt{\varepsilon}\left\langle\psi\psi_x v, r\right\rangle|.$$

Using Cauchy-Schwarz inequality and property (17) we get

$$|\Upsilon_2| \le 2\sqrt{\varepsilon}\||\psi\psi_x|^{\frac{1}{2}}v\|\||\psi\psi_x|^{\frac{1}{2}}r\| \le C\sqrt{\varepsilon}(\sigma h)^{-\frac{1}{2}}\||\psi\psi_x|^{\frac{1}{2}}v\|\|\psi r\|.$$

Then by the Young's inequality and the fact that $\beta_1 > 0$ and $\varepsilon < h$, we have

$$|\Upsilon_2| \le C\sqrt{\varepsilon}(\sigma h)^{-\frac{1}{2}}\beta_1^{-\frac{1}{2}}\Big[\beta_1\||\psi\psi_x|^{\frac{1}{2}}v\|^2 + \|\psi r\|^2\Big] \le C\sigma^{-\frac{1}{2}}\|\boldsymbol{\chi}\|^2_\star. \tag{28}$$

Analogously we can get

$$|\Upsilon_3| \le C\sigma^{-\frac{1}{2}}\|\boldsymbol{\chi}\|^2_\star. \tag{29}$$

Finally, noticing that $|\left\langle cv, \psi^2 v\right\rangle| \le C\|\psi v\|^2$ due to the boundedness of c, we obtain the conclusion (24) by collecting up the above estimates. □

Lemma 3.4. *Suppose $\varepsilon < h$. For any function $\boldsymbol{\chi}_h = (v_h, r_h, s_h) \in \boldsymbol{V_h}$, there holds*

$$B_h(\boldsymbol{\chi}_h, \Pi_h^\perp(\psi^2\boldsymbol{\chi}_h)) \le C\sigma^{-\frac{1}{2}}\|\boldsymbol{\chi}_h\|^2_\star, \tag{30}$$

where $\Pi_h^\perp\boldsymbol{\chi} = (\Pi_h^\perp v, \Pi_h^\perp r, \Pi_h^\perp s)$ for any function $\boldsymbol{\chi} = (v, r, s)$, and the bounding constant $C > 0$ is independent of $\sigma, h, x_0, y_0, \boldsymbol{\chi}_h$ and ε.

Proof. For notational convenience, we denote by

$$\Pi_h^{\perp}(\psi^2\boldsymbol{\chi}_h) = (\Pi_h^{\perp}(\psi^2 v_h), \Pi_h^{\perp}(\psi^2 r_h), \Pi_h^{\perp}(\psi^2 s_h)) = (\mathcal{E}_v, \mathcal{E}_r, \mathcal{E}_s).$$

It is followed from (10) that

$$B_h(\boldsymbol{\chi}_h, \Pi_h^{\perp}(\psi^2\boldsymbol{\chi}_h)) = \Phi_1 + \Phi_2 + \Phi_3 + \Phi_4, \tag{31}$$

where

$$\Phi_1 = \langle c v_h, \mathcal{E}_v\rangle + \langle r_h, \mathcal{E}_r\rangle + \langle s_h, \mathcal{E}_s\rangle, \tag{32a}$$

$$\Phi_2 = -\mathcal{H}_1(v_h, \mathcal{E}_v) - \mathcal{H}_2(v_h, \mathcal{E}_v), \tag{32b}$$

$$\Phi_3 = \sqrt{\varepsilon}\mathcal{K}_1^{\theta_1}(v_h, \mathcal{E}_r) + \sqrt{\varepsilon}\mathcal{L}_1^{\widetilde{\theta_1}}(r_h, \mathcal{E}_v), \tag{32c}$$

$$\Phi_4 = \sqrt{\varepsilon}\mathcal{K}_2^{\theta_2}(v_h, \mathcal{E}_s) + \sqrt{\varepsilon}\mathcal{L}_2^{\widetilde{\theta_2}}(s_h, \mathcal{E}_v), \tag{32d}$$

which will be estimated separately.

Using Cauchy-Schwarz inequality and the super-approximation property (21b), we get

$$\langle c v_h, \mathcal{E}_v\rangle \le C\|\psi v_h\|\|\psi^{-1}\mathcal{E}_v\| \le C\sigma^{-1}\|\psi v_h\|^2 \le C\sigma^{-1}\|\boldsymbol{\chi}_h\|_\star^2. \tag{33}$$

The estimate to the remaining two terms in Φ_1 are similar. So we obtain that $\Phi_1 \le C\sigma^{-1}\|\boldsymbol{\chi}_h\|_\star^2$.

Integrating by parts and noticing $\langle (v_h)_x, \mathcal{E}_v\rangle = 0$ due to the orthogonality of L^2 projection, after some trivial manipulation, we get that

$$\mathcal{H}_1(v_h, \mathcal{E}_v) = \sum_{j=1}^{N_y}\int_{J_j}\big[-\beta_1(v_h\mathcal{E}_v)^+_{\frac12,y} - \sum_{i=1}^{N_x-1}\beta_1([\![v_h]\!]\mathcal{E}_v^{\widetilde{\theta_1},y})_{i+\frac12,y} - \gamma_1(v_h\mathcal{E}_v)^-_{N_x+\frac12,y}\big]\mathrm{d}y.$$

Then using Cauchy-Schwarz inequality and the super-approximation property (21a), we have

$$\begin{aligned}\Big|\mathcal{H}_1(v_h, \mathcal{E}_v)\Big| &\le C\mathbb{J}_{x,\theta_1}(\psi v_h)\|\psi^{-1}\mathcal{E}_v\|_{\Gamma_h}\\ &\le C\sigma^{-\frac12}\mathbb{J}_{x,\theta_1}(\psi v_h)\||\psi\nabla\psi|^{\frac12}v_h\| \le C\sigma^{-\frac12}\|\boldsymbol{\chi}_h\|_\star^2.\end{aligned} \tag{34}$$

Similarly, we have $|\mathcal{H}_2(v_h, \mathcal{E}_v)| \le C\sigma^{-\frac12}\|\boldsymbol{\chi}_h\|_\star^2$ and thus $\Phi_2 \le C\sigma^{-\frac12}\|\boldsymbol{\chi}_h\|_\star^2$.

Now let's estimate Φ_3. Along the similar argument as that for $\mathcal{H}_1(v_h, \mathcal{E}_v)$, we have

$$\begin{aligned}&|\sqrt{\varepsilon}\mathcal{K}_1^{\theta_1}(v_h, \mathcal{E}_r)|\\ =&\Big|\sqrt{\varepsilon}\sum_{j=1}^{N_y}\int_{J_j}\big[-(v_h\mathcal{E}_r)^+_{\frac12,y} - \sum_{i=1}^{N_x-1}([\![v_h]\!]\mathcal{E}_r^{\widetilde{\theta_1},y})_{i+\frac12,y} + (v_h\mathcal{E}_r)^-_{N_x+\frac12,y}\big]\mathrm{d}y\Big|\\ \le& C\sqrt{\varepsilon}\mathbb{J}_{x,\theta_1}(\psi v_h)\|\psi^{-1}\mathcal{E}_r\|_{\Gamma_h}\\ \le& C\sqrt{\varepsilon}\mathbb{J}_{x,\theta_1}(\psi v_h)\big(h^{-\frac12}\sigma^{-1}\|\psi r_h\|\big) \le C\sigma^{-1}\|\boldsymbol{\chi}_h\|_\star^2,\end{aligned} \tag{35}$$

where the super-approximation property (21b) and $\varepsilon < h$ are used in the last line. In addition, by Lemma 2.1 and $\langle (r_h)_x, \mathcal{E}_v\rangle = 0$, we obtain

$$\begin{aligned}|\sqrt{\varepsilon}\mathcal{L}_1^{\widetilde{\theta_1}}(r_h, \mathcal{E}_v)| = |\sqrt{\varepsilon}\mathcal{K}_1^{\theta_1}(\mathcal{E}_v, r_h)| &= \Big|\sqrt{\varepsilon}\sum_{j=1}^{N_y}\int_{J_i}\sum_{i=1}^{N_x-1}\big(\mathcal{E}_v^{\theta_1,y}[\![r_h]\!]\big)_{i+\frac12,y}\mathrm{d}y\Big|\\ &\le C\sqrt{\varepsilon}\|\psi r_h\|_{\Gamma_h}\|\psi^{-1}\mathcal{E}_v\|_{\Gamma_h} \le C\sqrt{\varepsilon}\big(h^{-\frac12}\|\psi r_h\|\big)\big(\sigma^{-\frac12}\||\psi\nabla\psi|^{\frac12}v_h\|\big)\\ &\le C\sigma^{-\frac12}\|\boldsymbol{\chi}_h\|_\star^2,\end{aligned} \tag{36}$$

where Cauchy-Schwarz inequality, the inverse inequality (19) and the super -approximation property (21a), and $\varepsilon < h$ are used in the above inequalities. Thus we obtain $\Phi_3 \le C\sigma^{-\frac{1}{2}}\|\boldsymbol{\chi}_h\|_\star^2$. Analogously, $\Phi_4 \le C\sigma^{-\frac{1}{2}}\|\boldsymbol{\chi}_h\|_\star^2$.

Finally, collecting up the above estimates for Φ_1 to Φ_4, and noticing $\sigma^{-1} \le \sigma^{-\frac{1}{2}}$ due to $\sigma \ge 2$, we complete the proof of this lemma. □

3.4. Local stability conclusion. To establish the local stability conclusion, we follow [7] and assume that $F_h(\cdot)$ in (9) has a general form. Denote by

$$\|F_h(t)\|_\sharp = \sup_{\boldsymbol{\chi}_h \in \boldsymbol{V_h}} \frac{|F_h(t;\boldsymbol{\chi}_h)|}{\|\boldsymbol{\chi}_h\|_\sharp}, \quad \forall t \in (0,T], \tag{37}$$

where $\boldsymbol{\chi}_h = (v_h, r_h, s_h) \in \boldsymbol{V_h}$ and

$$\|\boldsymbol{\chi}_h\|_\sharp \equiv \Big[\|\psi^{-1}v_h\|^2 + \|\psi^{-1}r_h\|^2 + \|\psi^{-1}s_h\|^2 + \mathbb{J}^2_{x,\theta_1}(\psi^{-1}v_h) + \mathbb{J}^2_{y,\theta_2}(\psi^{-1}v_h)\Big]^{\frac{1}{2}}. \tag{38}$$

Along the same line as the proof of Lemma 3.3 in [7], we can set up the following local stability conclusion with the general form $F_h(\cdot)$.

Lemma 3.5. *Assume $\varepsilon < h$. If the parameter σ in the weight function* (15) *is large enough, then the solution of the LDG scheme* (9) *with the general form of $F_h(\cdot)$ satisfies*

$$\|\psi u_h(T)\|^2 \le C\Big\{\|\psi u_h(0)\|^2 + \int_0^T \|F_h(t)\|_\sharp^2 dt\Big\}, \tag{39}$$

where the bounding constant $C > 0$ is independent of σ, x_0, y_0, h and ε.

Applying Lemma 3.5 we can easily obtain the local stability for the considered LDG scheme (6), which is stated in the following theorem.

Theorem 3.1. *Assume $\varepsilon < h$. If the parameter σ in the weight function* (15) *is large enough, then the numerical solution of LDG scheme* (6) *satisfies*

$$\|\psi u_h(T)\|^2 \le C\|\psi u_h(0)\|^2 + C\int_0^T \Big[\|\psi f\|^2 + \|\psi g\|^2_{L^2(\Gamma)}\Big]\mathrm{d}t, \tag{40}$$

where the bounding constant $C > 0$ is independent of σ, x_0, y_0, h and ε.

Proof. Recalling the specific definition of $F_h(t;\boldsymbol{\chi}_h)$ in (11), applying Cauchy-Schwarz inequality and Young's inequality, we get that $F_h(t;\boldsymbol{\chi}_h) \le \Upsilon\Big[\|\psi f\|^2 + \|\psi g\|^2_{L^2(\Gamma)}\Big]^{\frac{1}{2}}$, where

$$\begin{aligned}\Upsilon &= C\Big\{\|\psi^{-1}v_h\|^2 + \varepsilon\|\psi^{-1}r_h\|^2_{\Gamma_h} + \varepsilon\|\psi^{-1}s_h\|^2_{\Gamma_h}\\ &\quad + \sum_{j=1}^{N_y}\int_{J_j}\big[\beta_1^2(\psi^{-1}v_h^+)^2_{\frac{1}{2},y} + \gamma_1^2(\psi^{-1}v_h^-)^2_{N_x+\frac{1}{2},y}\big]\mathrm{d}y\\ &\quad + \sum_{i=1}^{N_x}\int_{I_i}\big[\beta_2^2(\psi^{-1}v_h^+)^2_{x,\frac{1}{2}} + \gamma_2^2(\psi^{-1}v_h^-)^2_{x,N_y+\frac{1}{2}}\big]\mathrm{d}x\Big\}^{\frac{1}{2}}.\end{aligned} \tag{41}$$

Due to the inverse inequality (19) and $\varepsilon < h$, it is easy to derive that $\Upsilon \le C\|\boldsymbol{\chi}_h\|_\sharp$, which implies that

$$\|F_h(t)\|_\sharp \le C\Big[\|\psi f\|^2 + \|\psi g\|^2_{L^2(\Gamma)}\Big]^{\frac{1}{2}}. \tag{42}$$

So by Lemma 3.5 we get (40). □

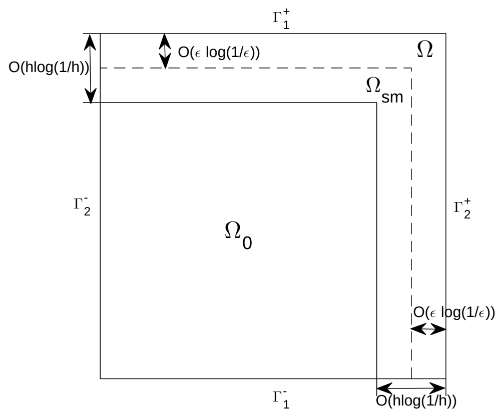

FIGURE 1. The square Ω and its sub-domains.

4. Local error estimate

The main goal of this section is to set up the double-optimal local error estimate of the LDG method (6) with GANF (7). To this end, we assume that the exact solution u can be decomposed in a precise way that is typical of the behaviors in solution of (1) observed when interior layers and corner singularities are excluded [17,20]. That is, there exists a positive constant M_1 independent of ε, such that

$$\left|D_x^i D_y^j D_t^\ell u(x,y,t)\right| \le M_1\Big[1+\frac{e^{-\beta_1(1-x)/\varepsilon}}{\varepsilon^i}\Big]\Big[1+\frac{e^{-\beta_2(1-y)/\varepsilon}}{\varepsilon^j}\Big] \tag{43}$$

for any nonnegative integers i, j and ℓ, and $(x,y,t)\in\overline{\Omega}\times(0,T]$. Let

$$\Omega_{\rm sm}=\Big(0,1-\rho_1\varepsilon\log\frac{1}{\varepsilon}\Big)\times\Big(0,1-\rho_2\varepsilon\log\frac{1}{\varepsilon}\Big),$$

with two positive constants $\rho_i\ge(k+2)/\beta_i$ for $i=1,2$ (see Figure 1). Then it follows from (43) that

$$\|D_x^i D_y^j D_t^\ell u\|_{L^2(\Omega_{\rm sm})}\le M_2, \tag{44a}$$

$$\|D_x^i D_y^j D_t^\ell u\|\le M_3[1+\varepsilon^{-i+\frac12}][1+\varepsilon^{-j+\frac12}], \tag{44b}$$

for any time $t\in(0,T]$ and $i+j+\ell\le k+2$, where both M_2 and M_3 are bounding constants independent of ε. For more details, please refer to [17,20].

We can obtain the following double-optimal local error estimate under these assumptions.

Theorem 4.1. *Assume that the exact solution u of singularly perturbed problem (1) satisfies (44). Let $u_h\in V_h$ be the numerical solution of the LDG scheme (6) with the generalized alternating numerical flux (7), where the finite element space V_h is made up of piecewise polynomials with degree at most $k\ge0$ in each variable, defined on quasi-uniform Cartesian mesh. Assume $0<\varepsilon<h\le h_0<1$, then there holds the following local error estimate*

$$\|u(T)-u_h(T)\|_{L^2(\Omega_0)}\le Ch^{k+1}, \tag{45}$$

where T is the final time and $\Omega_0=(0,1-C_1h\log\frac1h)\times(0,1-C_2h\log\frac1h)$ is the local domain (see Figure 1). Here $C, C_1, C_2>0$ are positive constants independent of h and ε.

Theorem 4.1 shows that the numerical layers are restricted in the narrow region nearby outflow boundaries with quasi-optimal width $\mathcal{O}(h\log(1/h))$. The similar result has been proved in [7] for one-dimensional case. For the two-dimensional case, although the proof line is similar, the extension is rather involved. We will show the detailed proof in the following subsections by using the 2-d GGR projections.

4.1. GGR projections. We will use three GGR projections in the later analysis. In what follows, the parameters $\theta_1 > 1/2$ and $\theta_2 > 1/2$ are arbitrary constants, which have special meaning on Γ.

(1) For any $z \in H^2(\Omega_h)$, the projection $\mathbb{P}_{\theta_1,\theta_2} z$ is the unique element in V_h such that

$$\int_{K_{ij}} (\mathbb{P}_{\theta_1,\theta_2} z) v_h \mathrm{d}x\mathrm{d}y = \int_{K_{ij}} z v_h \mathrm{d}x\mathrm{d}y, \tag{46a}$$

$$\int_{J_j} \big((\mathbb{P}_{\theta_1,\theta_2} z)^{\theta_1,y} v_h\big)_{i+\frac12,y} \mathrm{d}y = \int_{J_j} \big(z^{\theta_1,y} v_h\big)_{i+\frac12,y} \mathrm{d}y, \tag{46b}$$

$$\int_{I_i} \big((\mathbb{P}_{\theta_1,\theta_2} z)^{x,\theta_2} v_h\big)_{x,j+\frac12} \mathrm{d}x = \int_{I_i} \big(z^{x,\theta_2} v_h\big)_{x,j+\frac12} \mathrm{d}x, \tag{46c}$$

$$\big(\mathbb{P}_{\theta_1,\theta_2} z\big)^{\theta_1,\theta_2}_{i+\frac12,j+\frac12} = z^{\theta_1,\theta_2}_{i+\frac12,j+\frac12}, \tag{46d}$$

hold for any $v_h \in \mathcal{Q}^{k-1}(K_{ij})$ and $i = 1, 2, \cdots, N_x$, $j = 1, 2, \cdots, N_y$. Here and below the values of test function v_h are taken from inside of each element. In (46), $z^{\theta_1,y}_{i+\frac12,y}$ and $z^{x,\theta_2}_{x,j+\frac12}$ are weighted averages on the element interfaces defined in (4b), and $z^{\theta_1,\theta_2}_{i+\frac12,j+\frac12}$ is the weighted average at the corner point $(x_{i+\frac12}, y_{j+\frac12})$, which is defined as

$$\begin{aligned} z^{\theta_1,\theta_2}_{i+\frac12,j+\frac12} =& \theta_1\theta_2 z(x^-_{i+\frac12}, y^-_{j+\frac12}) + \theta_1\widetilde{\theta}_2 z(x^-_{i+\frac12}, y^+_{j+\frac12}) \\ &+ \widetilde{\theta}_1\theta_2 z(x^+_{i+\frac12}, y^-_{j+\frac12}) + \widetilde{\theta}_1\widetilde{\theta}_2 z(x^+_{i+\frac12}, y^+_{j+\frac12}). \end{aligned}$$

Noting that in the cases $i = N_x$ and $j = N_y$, the parameters $\theta_1 = 1$ and $\theta_2 = 1$, respectively.

(2) For any function $z \in H^1(\Omega_h)$, the projection $\mathbb{Q}_{\widetilde{\theta}_1,\frac12} z \in V_h$ satisfies

$$\int_{K_{ij}} \mathbb{Q}_{\widetilde{\theta}_1,\frac12} z (v_h)_x \mathrm{d}x\mathrm{d}y = \int_{K_{ij}} z (v_h)_x \mathrm{d}x\mathrm{d}y, \tag{47a}$$

$$\int_{J_j} \big((\mathbb{Q}_{\widetilde{\theta}_1,\frac12} z)^{\widetilde{\theta}_1,y} v_h\big)_{i-\frac12,y} \mathrm{d}y = \int_{J_j} \big(z^{\widetilde{\theta}_1,y} v_h\big)_{i-\frac12,y} \mathrm{d}y, \tag{47b}$$

for any $v_h \in \mathcal{Q}^k(K_{ij})$ and any $i = 1, 2, \ldots, N_x$, $j = 1, 2, \ldots, N_y$. Here the parameter $\theta_1 = 1$ at the domain boundary $(x_{\frac12}, y)$ for $y \in J_j$.

(3) For any function $z \in H^1(\Omega_h)$, the projection $\mathbb{Q}_{\frac12,\widetilde{\theta}_2} z \in V_h$ satisfies

$$\int_{K_{ij}} \mathbb{Q}_{\frac12,\widetilde{\theta}_2} z (v_h)_y \mathrm{d}x\mathrm{d}y = \int_{K_{ij}} z (v_h)_y \mathrm{d}x\mathrm{d}y, \tag{48a}$$

$$\int_{I_i} \big((\mathbb{Q}_{\frac12,\widetilde{\theta}_2} z)^{x,\widetilde{\theta}_2} v_h\big)_{x,j-\frac12} \mathrm{d}x = \int_{I_i} \big(z^{x,\widetilde{\theta}_2} v_h\big)_{x,j-\frac12} \mathrm{d}x, \tag{48b}$$

for any $v_h \in \mathcal{Q}^k(K_{ij})$, and any $i = 1, 2, \ldots, N_x$, $j = 1, 2, \ldots, N_y$. Here the parameter $\theta_2 = 1$ at the domain boundary $(x, y_{\frac12})$ for $x \in I_i$.

Lemma 4.1. *Each of the GGR projections $\mathbb{P}_{\theta_1,\theta_2}$, $\mathbb{Q}_{\widetilde{\theta}_1,\frac{1}{2}}$ and $\mathbb{Q}_{\frac{1}{2},\widetilde{\theta}_2}$ exists uniquely.*

Proof. The proof is the similar as that in [4,7]. For the completeness of this paper, we would like to present the proof for $\mathbb{P}_{\theta_1,\theta_2}$ as an example.

In fact, we only need to show the unique existence of $E = \mathbb{P}_{\theta_1,\theta_2} z - \Pi_h z$ for any $z \in H^2(\Omega_h)$, since we have known that the local L^2-projection $\Pi_h z$ exists uniquely. It follows from (46) that

$$\int_{K_{ij}} E v_h \mathrm{d}x\mathrm{d}y = 0, \tag{49a}$$

$$\int_{J_j} \left(E^{\theta_1,y} v_h\right)_{i+\frac{1}{2},y} \mathrm{d}y = \int_{J_j} \left(\epsilon^{\theta_1,y} v_h\right)_{i+\frac{1}{2},y} \mathrm{d}y, \tag{49b}$$

$$\int_{I_i} \left(E^{x,\theta_2} v_h\right)_{x,j+\frac{1}{2}} \mathrm{d}x = \int_{I_i} \left(\epsilon^{x,\theta_2} v_h\right)_{x,j+\frac{1}{2}} \mathrm{d}x, \tag{49c}$$

$$E^{\theta_1,\theta_2}_{i+\frac{1}{2},j+\frac{1}{2}} = \epsilon^{\theta_1,\theta_2}_{i+\frac{1}{2},j+\frac{1}{2}}, \tag{49d}$$

for any $v_h \in \mathcal{Q}^{k-1}(K_{ij})$ and any $i = 1, 2, \ldots, N_x$ and $j = 1, 2, \ldots, N_y$, where

$$\epsilon = z - \Pi_h z$$

is already known. Since $E \in V_h$, we have the orthogonal expansion

$$E(x,y)|_{K_{ij}} = \sum_{\ell_1=0}^{k} \sum_{\ell_2=0}^{k} \alpha_{i,j}^{\ell_1,\ell_2} P^i_{\ell_1}(x) P^j_{\ell_2}(y).$$

Here

$$P^i_{\ell_1}(x) = \widehat{P}_{\ell_1}(\hat{x}) \qquad \text{and} \qquad P^j_{\ell_2}(y) = \widehat{P}_{\ell_2}(\hat{y})$$

with $\widehat{P}_\ell$ representing the standard Legendre polynomial of degree ℓ on $[-1,1]$, and the affine mapping $\hat{x} = 2(x - x_i)/h_x^i$ and $\hat{y} = 2(y - y_j)/h_y^j$, where $x_i = (x_{i-\frac{1}{2}} + x_{i+\frac{1}{2}})/2$, $y_j = (y_{j-\frac{1}{2}} + y_{j+\frac{1}{2}})/2$ and $h_x^i = x_{i+\frac{1}{2}} - x_{i-\frac{1}{2}}$, $h_y^j = y_{j+\frac{1}{2}} - y_{j-\frac{1}{2}}$.

Owing to (49a) and the orthogonality of Legendre polynomials, it is easy to show that

$$E|_{K_{ij}} = E_1 + E_2 + E_0,$$

where

$$E_1 = \sum_{\ell_2=0}^{k-1} \alpha_{i,j}^{k,\ell_2} P^i_k(x) P^j_{\ell_2}(y), \tag{50a}$$

$$E_2 = \sum_{\ell_1=0}^{k-1} \alpha_{i,j}^{\ell_1,k} P^i_{\ell_1}(x) P^j_k(y), \tag{50b}$$

$$E_0 = \alpha_{i,j}^{k,k} P^i_k(x) P^j_k(y). \tag{50c}$$

The unique existence of E can be verified by showing the same conclusion for each component. This purpose can be achieved by direct manipulations. Before showing the details, we would like to introduce a couple of notations

$$\vec{w}_{x,j}^{\ell_1,\ell_2} = (w_{1,j}^{\ell_1,\ell_2}, w_{2,j}^{\ell_1,\ell_2}, \cdots, w_{N_x,j}^{\ell_1,\ell_2})^\top \quad \text{and} \quad \vec{w}_{i,y}^{\ell_1,\ell_2} = (w_{i,1}^{\ell_1,\ell_2}, w_{i,2}^{\ell_1,\ell_2}, \cdots, w_{i,N_y}^{\ell_1,\ell_2})^\top$$

for any w and any $i = 1, 2, \cdots, N_x$, $j = 1, 2, \cdots, N_y$ and $\ell_1, \ell_2 = 0, 1, \cdots, k$.

Then due to (49b), we can solve E_1 from the linear system

$$\mathbb{A}_{N_x} \vec{\alpha}_{x,j}^{k,\ell_2} = \vec{b}_{x,j}^{k,\ell_2} \tag{51}$$

for any $\ell_2 = 0, 1, \ldots, k-1$ and $j = 1, 2, \ldots, N_y$, where $\mathbb{A}_{N_x}$ is a $N_x \times N_x$ matrix, which is given by

$$\mathbb{A}_{N_x} = \begin{bmatrix} \theta_1 & \widetilde{\theta}_1(-1)^k & & & \\ & \theta_1 & \widetilde{\theta}_1(-1)^k & & \\ & & \ddots & \ddots & \\ & & & \theta_1 & \widetilde{\theta}_1(-1)^k \\ & & & & 1 \end{bmatrix} \tag{52}$$

and each component of $\vec{b}^{k,\ell_2}_{x,j}$ is given by

$$b^{k,\ell_2}_{i,j} = \frac{1}{\|P^j_{\ell_2}(y)\|^2_{L^2(J_j)}} \int_{J_j} \left(\epsilon^{\theta_1,y} P^j_{\ell_2}(y)\right)_{i+\frac{1}{2},y} \mathrm{d}y, \quad \text{for } i = 1, 2, \ldots, N_x. \tag{53}$$

Since $\det(\mathbb{A}_{N_x}) = \theta_1^{N_x-1}$ and $\theta_1 > \frac{1}{2}$, we can conclude that $\mathbb{A}_{N_x}$ is invertible and thus E_1 is determined uniquely.

Analogously, we can prove that E_2 is also determined uniquely due to (49c). The corresponding linear system is

$$\mathbb{A}_{N_y} \vec{\alpha}^{\ell_1,k}_{i,y} = \vec{b}^{\ell_1,k}_{i,y} \tag{54}$$

for any $\ell_1 = 0, 1, \ldots, k-1$ and $i = 1, 2, \ldots, N_x$, where $\mathbb{A}_{N_y}$ is a $N_y \times N_y$ matrix, which has the similar structure as $\mathbb{A}_{N_x}$, just replacing θ_1 with θ_2, and each component of $\vec{b}^{\ell_1,k}_{i,y}$ is

$$b^{\ell_1,k}_{i,j} = \frac{1}{\|P^i_{\ell_1}(x)\|^2_{L^2(I_i)}} \int_{I_i} \left(\epsilon^{x,\theta_2} P^i_{\ell_1}(x)\right)_{x,j+\frac{1}{2}} \mathrm{d}x, \quad \text{for } j = 1, 2, \ldots, N_y. \tag{55}$$

The undetermined coefficients $\alpha^{k,k}_{i,j}$ in the last component E_0 can be solved from the last condition (49d) which forms the linear system

$$\left(\mathbb{A}_{N_x} \otimes \mathbb{A}_{N_y}\right) \vec{\alpha}^{k,k} = \vec{b}^{k,k}, \tag{56}$$

where $\vec{\alpha}^{k,k} = \begin{pmatrix} \vec{\alpha}^{k,k}_{x,1} \\ \vec{\alpha}^{k,k}_{x,2} \\ \vdots \\ \vec{\alpha}^{k,k}_{x,N_y} \end{pmatrix}$ and $\vec{b}^{k,k} = \begin{pmatrix} \vec{b}^{k,k}_{x,1} \\ \vec{b}^{k,k}_{x,2} \\ \vdots \\ \vec{b}^{k,k}_{x,N_y} \end{pmatrix}$, with

$$b^{k,k}_{i,j} = (\epsilon - E_1 - E_2)^{\theta_1,\theta_2}_{i+\frac{1}{2},j+\frac{1}{2}}, \quad \text{for } i = 1, \ldots, N_x, \; j = 1, \ldots, N_y. \tag{57}$$

By the elemental properties of Kronecker product of matrices [12], we can obtain that

$$\det(\mathbb{A}_{N_x} \otimes \mathbb{A}_{N_y}) = \det(\mathbb{A}_{N_x})^{N_y} \det(\mathbb{A}_{N_y})^{N_x} > 0,$$

for $\theta_1 > \frac{1}{2}$ and $\theta_2 > \frac{1}{2}$, so E_0 is also determined uniquely. This finishes the proof of this lemma. □

Following [4], we can establish the optimal approximation property of the above GGR projection under the trivial weight function $\psi = 1$. However, to carry out the local error estimate, we need to set up the sharp approximation property of the GGR projections with the weight function (15). Here we follow the proof line of [7], and investigate the structure of coefficient matrix with the weight function. To bound the weighted approximation error at the corner points, we employ some properties of the tensor product of matrices.

Lemma 4.2. *Let $\mathbb{W}_h$ be either of the GGR projections $\mathbb{P}_{\theta_1,\theta_2}$, $\mathbb{Q}_{\widetilde{\theta}_1,\frac{1}{2}}$ or $\mathbb{Q}_{\frac{1}{2},\widetilde{\theta}_2}$ with $\theta_1 > \frac{1}{2}$ and $\theta_2 > \frac{1}{2}$. Assume $z \in H^{s+1}(\Omega_h) \cap H^2(\Omega_h)$ with $s \geq 0$, the GGR projection error $\mathbb{W}_h^{\perp} z = z - \mathbb{W}_h z$ satisfies*

$$\begin{aligned}&\|\psi \mathbb{W}_h^{\perp} z\| + h^{\frac{1}{2}} \|\psi \mathbb{W}_h^{\perp} z\|_{\Gamma_h}\\ &\leq Ch^{\min(k,s)+1}\Big[|z|_{\psi,s+1} + \big(|\widetilde{\theta}_1\theta_1^{-1}|^{\sigma} + |\widetilde{\theta}_2\theta_2^{-1}|^{\sigma}\big)|z|_{s+1}\Big],\end{aligned} \tag{58}$$

where $\sigma \geq 2$ is the parameter in the weight function ψ given by (15)*, and the bounding constant $C = C(\theta_1,\theta_2) > 0$ is independent of σ, x_0, y_0, z and h.*

Proof. We still take $\mathbb{W}_h = \mathbb{P}_{\theta_1,\theta_2}$ as an example and keep the same notations as that in the proof of Lemma 4.1. To prove this lemma, we just need to show

$$\|\psi E\|^2 + h\|\psi E\|^2_{\Gamma_h} \leq Ch^{2\min(k,s)+2}\Big[|z|^2_{\psi,s+1} + \big(|\widetilde{\theta}_1\theta_1^{-1}|^{2\sigma} + |\widetilde{\theta}_2\theta_2^{-1}|^{2\sigma}\big)|z|^2_{s+1}\Big], \tag{59}$$

due to the approximation property (20). The proof will be proceeded in the following three steps.

Step 1. We would like to show that

$$\|\psi E_1\|^2 + h\|\psi E_1\|^2_{\Gamma_h} \leq Ch^{2\min(k,s)+2}\Big[|z|^2_{\psi,s+1} + |\widetilde{\theta}_1\theta_1^{-1}|^{2\sigma}|z|^2_{s+1}\Big]. \tag{60}$$

To this end, we follow the similar arguments as those given in [7], where one-dimensional case was discussed. Denote $\psi_{ij} = \max_{(x,y)\in\overline{K}_{ij}} \psi(x,y)$ and define $\beta^{k,\ell_2}_{i,j} = \psi_{ij}\alpha^{k,\ell_2}_{i,j}$ for any i,j and $\ell_2 = 0,1,\cdots,k-1$, where $\alpha^{k,\ell_2}_{i,j}$ is determined by the linear system (51). Owing to (50a) and the boundedness of Legendre polynomials, we can obtain

$$\begin{aligned}\|\psi E_1\|^2 + h\|\psi E_1\|^2_{\Gamma_h} &\leq Ch^2 \sum_{i=1}^{N_x}\sum_{j=1}^{N_y}\sum_{\ell_2=0}^{k-1}\Big[\alpha^{k,\ell_2}_{i,j}\psi_{ij}\Big]^2 = Ch^2\sum_{\ell_2=0}^{k-1}\sum_{j=1}^{N_y}\sum_{i=1}^{N_x}\Big[\beta^{k,\ell_2}_{i,j}\Big]^2\\ &= Ch^2\sum_{\ell_2=0}^{k-1}\sum_{j=1}^{N_y}\|\vec{\beta}^{k,\ell_2}_{x,j}\|_2^2,\end{aligned} \tag{61}$$

where $\|\vec{w}\|_2$ means the l_2 norm of vector $\vec{w}$. To bound $\|\vec{\beta}^{k,\ell_2}_{x,j}\|_2$ sharply, we follow [7] to split $\mathbb{A}^{-1}_{N_x}$ into two parts, namely

$$\mathbb{A}^{-1}_{N_x} = \mathbb{B}_{N_x} + \mathbb{C}_{N_x}, \tag{62}$$

where

$$\mathbb{B}_{N_x} = \frac{1}{\theta_1}\left[\begin{array}{cccc|cccc} 1 & \zeta_1 & \cdots & \zeta_1^{\sigma-1} & & & & \\ & 1 & \cdots & \zeta_1^{\sigma-2} & \zeta_1^{\sigma-1} & & & \\ & & \ddots & \ddots & \ddots & \ddots & & \\ & & & 1 & \zeta_1 & \cdots & \zeta_1^{\sigma-1} & \\ \hline & & & & 1 & \cdots & \zeta_1^{\sigma-2} & \theta_1\zeta_1^{\sigma-1} \\ & \mathbf{0} & & & & \ddots & \vdots & \vdots \\ & & & & & & 1 & \theta_1\zeta_1 \\ & & & & & & & \theta_1 \end{array}\right], \tag{63}$$

and

$$
\mathbb{C}_{N_x}=\frac{1}{\theta_1}\left[\begin{array}{cccc|cccc}
0 & & & & \zeta_1^{\sigma} & \cdots & \zeta_1^{N_x-2} & \theta_1\zeta_1^{N_x-1}\\
 & 0 & & & & \zeta_1^{\sigma} & \cdots & \theta_1\zeta_1^{N_x-2}\\
 & & \ddots & & & & \ddots & \vdots\\
 & & & 0 & 0 & & & \theta_1\zeta_1^{\sigma}\\
\hline
 & & & & 0 & & & \\
 & & & & & 0 & & \\
 & \multicolumn{2}{c}{\mathbf{0}} & & & & \ddots & \\
 & & & & & & & 0
\end{array}\right], \tag{64}
$$

with $\zeta_1=(-1)^{k+1}\widetilde{\theta}_1\theta_1^{-1}$.

Define $\Psi_{x,j}=\mathrm{diag}(\psi_{1j},\psi_{2j},\ldots,\psi_{N_xj})$, then we have

$$
\vec{\beta}_{x,j}^{k,\ell_2}=\Psi_{x,j}\vec{\alpha}_{x,j}^{k,\ell_2}=\Psi_{x,j}\mathbb{A}_{N_x}^{-1}\vec{b}_{x,j}^{k,\ell_2}=(\Psi_{x,j}\mathbb{B}_{N_x}\Psi_{x,j}^{-1})(\Psi_{x,j}\vec{b}_{x,j}^{k,\ell_2})+(\Psi_{x,j}\mathbb{C}_{N_x})\vec{b}_{x,j}^{k,\ell_2}. \tag{65}
$$

Since the matrix $\Psi_{x,j}\mathbb{B}_{N_x}\Psi_{x,j}^{-1}$ has the same structure about the non-zero data as $\mathbb{B}_{N_x}$, and there is an additional multiplier $\psi_{i_1,j}/\psi_{i_2,j}$ among their elements at the i_1-th row and i_2-th column which satisfies

$$
\Big|\frac{\psi_{i_1,j}}{\psi_{i_2,j}}\Big|\le\max_{|x_2-x_1|\le\sigma h}\Big|\frac{\psi(x_1,y)}{\psi(x_2,y)}\Big|\le C,\quad 0\le i_2-i_1\le\sigma-1,\ \forall y. \tag{66}
$$

By the property (17), we have

$$
\|\Psi_{x,j}\mathbb{B}_{N_x}\Psi_{x,j}^{-1}\|_2^2\le C\|\mathbb{B}_{N_x}\|_2^2\le C. \tag{67}
$$

In addition, by Cauchy-Schwarz inequality, the approximation property of L^2 projection, and the property (18), we have

$$
\begin{aligned}
\|\Psi_{x,j}\vec{b}_{x,j}^{k,\ell_2}\|_2^2&=\sum_{i=1}^{N_x}\Big[b_{i,j}^{k,\ell_2}\psi_{ij}\Big]^2\le\sum_{i=1}^{N_x}\psi_{ij}^2\left(\frac{\|\epsilon_{i+\frac12,y}^{\theta_1,y}\|_{L^2(J_j)}}{\|P_{\ell_2}^j(y)\|_{L^2(J_j)}}\right)^2\\
&\le C\sum_{i=1}^{N_x}\psi_{ij}^2\|\epsilon\|_{L^\infty(\mathcal{O}_{ij})}^2\le Ch^{\min(2k,2s)}\sum_{i=1}^{N_x}\psi_{ij}^2|z|_{s+1,\mathcal{O}_{ij}}^2\\
&\le Ch^{\min(2k,2s)}\sum_{i=1}^{N_x}|z|_{\psi,s+1,K_{ij}}^2,
\end{aligned} \tag{68}
$$

where $\mathcal{O}_{ij}$ is the neighbor elements besides the element boundary $(x_{i+\frac12},y)$ in horizontal direction, which has at most two elements. For the trivial weight function $\psi=1$, the above inequality is expressed in the form

$$
\|\vec{b}_{x,j}^{k,\ell_2}\|_2^2=\sum_{i=1}^{N_x}\Big[b_{i,j}^{k,\ell_2}\Big]^2\le Ch^{\min(2k,2s)}\sum_{i=1}^{N_x}|z|_{s+1,K_{ij}}^2.
$$

Moreover, following [7] we can get easily that

$$
\|\mathbb{C}_{N_x}\|_2^2\le\|\mathbb{C}_{N_x}\|_\infty\|\mathbb{C}_{N_x}\|_1\le C|\zeta_1|^{2\sigma},\quad \|\Psi_{x,j}\|_2^2\le\|\Psi_{x,j}\|_\infty\|\Psi_{x,j}\|_1\le C. \tag{69}
$$

Collecting up the above estimates, we obtain that

$$
\begin{aligned}
\|\vec{\beta}_{x,j}^{k,\ell_2}\|_2^2&\le\|\Psi_{x,j}\mathbb{B}_{N_x}\Psi_{x,j}^{-1}\|_2^2\|\Psi_{x,j}\vec{b}_{x,j}^{k,\ell_2}\|_2^2+\|\Psi_{x,j}\|_2^2\|\mathbb{C}_{N_x}\|_2^2\|\vec{b}_{x,j}^{k,\ell_2}\|_2^2\\
&\le Ch^{2\min(k,s)}\Big\{\sum_{i=1}^{N_x}|z|_{\psi,s+1,K_{ij}}^2+|\zeta_1|^{2\sigma}\sum_{i=1}^{N_x}|z|_{s+1,K_{ij}}^2\Big\}.
\end{aligned} \tag{70}
$$

As a result, we obtain the conclusion (60) by (61) and (70).

Step 2. Repeating the same arguments as Step 1, we can prove

$$\|\psi E_2\|^2 + h\|\psi E_2\|^2_{\Gamma_h} \le Ch^{2\min(k,s)+2}\Big[|z|^2_{\psi,s+1} + |\widetilde{\theta}_2\theta_2^{-1}|^{2\sigma}|z|^2_{s+1}\Big]. \tag{71}$$

In this process, the matrix division

$$\mathbb{A}^{-1}_{N_y} = \mathbb{B}_{N_y} + \mathbb{C}_{N_y} \tag{72}$$

is used, where $\mathbb{B}_{N_y}$ and $\mathbb{C}_{N_y}$ have the similar structures as $\mathbb{B}_{N_x}$ and $\mathbb{C}_{N_x}$ defined in (63) and (64), just replacing θ_1 with θ_2, ζ_1 with $\zeta_2 = (-1)^{k+1}\widetilde{\theta}_2\theta_2^{-1}$ and N_x with N_y.

And similarly as (70) we can obtain

$$\|\vec{\beta}^{\ell_1,k}_{i,y}\|^2_2 \le Ch^{2\min(k,s)}\Big\{\sum_{j=1}^{N_y}|z|^2_{\psi,s+1,K_{ij}} + |\zeta_2|^{2\sigma}\sum_{j=1}^{N_y}|z|^2_{s+1,K_{ij}}\Big\}, \tag{73}$$

where $\vec{\beta}^{\ell_1,k}_{i,y} = \Psi_{i,y}\vec{\alpha}^{\ell_1,k}_{i,y}$, with $\Psi_{i,y} = \mathrm{diag}(\psi_{i1}, \psi_{i2}, \ldots, \psi_{iN_y})$ and $\vec{\alpha}^{\ell_1,k}_{i,y}$ determined by (54).

Step 3. The main difficulty is to show

(74)

$$\|\psi E_0\|^2 + h\|\psi E_0\|^2_{\Gamma_h} \le Ch^{2\min(k,s)+2}\Big[|z|^2_{\psi,s+1} + \big(|\widetilde{\theta}_1\theta_1^{-1}|^{2\sigma} + |\widetilde{\theta}_2\theta_2^{-1}|^{2\sigma}\big)|z|^2_{s+1}\Big].$$

It follows from (50c) that

$$\|\psi E_0\|^2 + h\|\psi E_0\|^2_{\Gamma_h} \le Ch^2\sum_{i=1}^{N_x}\sum_{j=1}^{N_y}\Big[\alpha^{k,k}_{i,j}\psi_{ij}\Big]^2 = Ch^2\sum_{i=1}^{N_x}\sum_{j=1}^{N_y}\Big[\beta^{k,k}_{i,j}\Big]^2 = Ch^2\|\vec{\beta}^{k,k}\|^2_2,$$

where $\vec{\beta}^{k,k} = \Psi\vec{\alpha}^{k,k}$, with $\vec{\alpha}^{k,k}$ determined by (56) and $\Psi = \mathrm{diag}(\Psi_{x,1}, \Psi_{x,2}, \cdots, \Psi_{x,N_y})$.

Thanks to (62), (72), and the elemental properties of Kronecker product of matrices [12], we have

$$\begin{aligned}
\vec{\beta}^{k,k} &= \Psi(\mathbb{A}_{N_x}\otimes\mathbb{A}_{N_y})^{-1}\vec{b}^{k,k} = \Psi(\mathbb{A}^{-1}_{N_x}\otimes\mathbb{A}^{-1}_{N_y})\vec{b}^{k,k}\\
&= \Psi\Big[\mathbb{B}_{N_x}\otimes\mathbb{B}_{N_y} + \mathbb{B}_{N_x}\otimes\mathbb{C}_{N_y} + \mathbb{C}_{N_x}\otimes\mathbb{B}_{N_y} + \mathbb{C}_{N_x}\otimes\mathbb{C}_{N_y}\Big]\vec{b}^{k,k}\\
&= \Big(\Psi\mathbb{B}_{N_x}\otimes\mathbb{B}_{N_y}\Psi^{-1}\Big)\Big(\Psi\vec{b}^{k,k}\Big)\\
&\quad + \Psi\Big[\mathbb{B}_{N_x}\otimes\mathbb{C}_{N_y} + \mathbb{C}_{N_x}\otimes\mathbb{B}_{N_y} + \mathbb{C}_{N_x}\otimes\mathbb{C}_{N_y}\Big]\vec{b}^{k,k}.
\end{aligned}$$

Since the matrix $\Psi(\mathbb{B}_{N_x}\otimes\mathbb{B}_{N_y})\Psi^{-1}$ has the same structure about the non-zero data as $\mathbb{B}_{N_x}\otimes\mathbb{B}_{N_y}$, and there is an additional multiplier $\psi_{i_1,j_1}/\psi_{i_2,j_2}$ among their elements at the $(j_1(N_y-1)+i_1)$-th row and $(j_2(N_y-1)+i_2)$-th column, which satisfies

$$\Big|\frac{\psi_{i_1,j_1}}{\psi_{i_2,j_2}}\Big| \le \max_{\substack{|x_2-x_1|\le\sigma h\\ |y_2-y_1|\le\sigma h}}\Big|\frac{\psi(x_1,y_1)}{\psi(x_2,y_2)}\Big| \le C, \tag{75}$$

for any $0 \le i_2 - i_1 \le \sigma - 1$ and $0 \le j_2 - j_1 \le \sigma - 1$, due to the property (17), we have

$$\|\Psi(\mathbb{B}_{N_x}\otimes\mathbb{B}_{N_y})\Psi^{-1}\|^2_2 \le C\|\mathbb{B}_{N_x}\otimes\mathbb{B}_{N_y}\|^2_2 \le C\|\mathbb{B}_{N_x}\|^2_2\|\mathbb{B}_{N_y}\|^2_2 \le C.$$

In addition, by (57), (50) and the similar argument as (68), we can prove that

$$\|\Psi\vec{b}^{k,k}\|_2^2 = \sum_{i=1}^{N_x}\sum_{j=1}^{N_y}(\psi_{ij}b_{ij}^{k,k})^2$$
$$\le C\sum_{i=1}^{N_x}\sum_{j=1}^{N_y}\psi_{ij}^2\|\epsilon\|_{L^\infty(\mathcal{O}_{ij})}^2 + C\sum_{i=1}^{N_x}\sum_{j=1}^{N_y}\sum_{\ell_2=0}^{k-1}\left[\alpha_{i,j}^{k,\ell_2}\psi_{ij}\right]^2 + C\sum_{i=1}^{N_x}\sum_{j=1}^{N_y}\sum_{\ell_1=0}^{k-1}\left[\alpha_{i,j}^{\ell_1,k}\psi_{ij}\right]^2$$
$$\le Ch^{\min(2k,2s)}\sum_{i=1}^{N_x}\sum_{j=1}^{N_y}|z|_{\psi,s+1,K_{ij}}^2 + C\sum_{\ell_2=0}^{k-1}\sum_{j=1}^{N_y}\|\vec{\beta}_{x,j}^{k,\ell_2}\|_2^2 + C\sum_{\ell_1=0}^{k-1}\sum_{i=1}^{N_x}\|\vec{\beta}_{i,y}^{\ell_1,k}\|_2^2,$$

where $\mathcal{O}_{ij}$ is the neighbor elements around the corner point $(x_{i+\frac{1}{2}}, y_{j+\frac{1}{2}})$, which has at most four elements.

Thus, by (70) and (73), we get

$$\|\Psi\vec{b}^{k,k}\|_2^2 \le Ch^{2\min(k,s)}\Big[|z|_{\psi,s+1}^2 + \big(|\zeta_1|^{2\sigma} + |\zeta_2|^{2\sigma}\big)|z|_{s+1}^2\Big]. \tag{76}$$

Note that the conclusion holds for the trivial weight function $\psi = 1$ in the form

$$\|\vec{b}^{k,k}\|_2^2 \le Ch^{2\min(k,s)}|z|_{s+1}^2,$$

since the trivial weight function $\psi = 1$ can be expressed as the form (15) with steepness $\sigma = +\infty$. In addition, we can easily see that $\|\Psi\|_2^2 \le C$, and

$$\|\mathbb{C}_{N_x}\otimes\mathbb{B}_{N_y}\|_2^2 \le \|\mathbb{C}_{N_x}\|_2^2\cdot\|\mathbb{B}_{N_y}\|_2^2 \le C|\zeta_1|^{2\sigma}, \tag{77}$$
$$\|\mathbb{B}_{N_x}\otimes\mathbb{C}_{N_y}\|_2^2 \le \|\mathbb{B}_{N_x}\|_2^2\cdot\|\mathbb{C}_{N_y}\|_2^2 \le C|\zeta_2|^{2\sigma}, \tag{78}$$
$$\|\mathbb{C}_{N_x}\otimes\mathbb{C}_{N_y}\|_2^2 \le \|\mathbb{C}_{N_x}\|_2^2\cdot\|\mathbb{C}_{N_y}\|_2^2 \le C|\zeta_1|^{2\sigma}|\zeta_2|^{2\sigma}. \tag{79}$$

Therefore we get that

$$\begin{aligned}\|\vec{\beta}^{k,k}\|_2^2 &\le \|\Psi\mathbb{B}_{N_x}\otimes\mathbb{B}_{N_y}\Psi^{-1}\|_2^2\|\Psi\vec{b}^{k,k}\|_2^2\\ &\quad + \|\Psi\|_2^2\Big[\|\mathbb{C}_{N_x}\otimes\mathbb{B}_{N_y}\|_2^2 + \|\mathbb{B}_{N_x}\otimes\mathbb{C}_{N_y}\|_2^2 + \|\mathbb{C}_{N_x}\otimes\mathbb{C}_{N_y}\|_2^2\Big]\|\vec{b}^{k,k}\|_2^2\\ &\le Ch^{2\min(k,s)}\Big[|z|_{\psi,s+1}^2 + \big(|\zeta_1|^{2\sigma} + |\zeta_2|^{2\sigma}\big)|z|_{s+1}^2\Big].\end{aligned}$$

This results in the assertion (74).

Finally, collecting up the above estimates leads to (59) and we complete the whole proof. □

4.2. Proof of Theorem 4.1. In this subsection, we are going to prove Theorem 4.1. As the standard treatment in the finite element analysis, we consider the splitting of numerical error $\boldsymbol{e} = (u - u_h, p - p_h, q - q_h) = \boldsymbol{\eta} - \boldsymbol{\xi}$ with

$$\boldsymbol{\eta} = (\eta_u, \eta_p, \eta_q) = (u - \mathbb{P}_{\theta_1,\theta_2}u, p - \mathbb{Q}_{\widetilde{\theta}_1,\frac{1}{2}}p, q - \mathbb{Q}_{\frac{1}{2},\widetilde{\theta}_2}q), \tag{80a}$$
$$\boldsymbol{\xi} = (\xi_u, \xi_p, \xi_q) = (u_h - \mathbb{P}_{\theta_1,\theta_2}u, p_h - \mathbb{Q}_{\widetilde{\theta}_1,\frac{1}{2}}p, q_h - \mathbb{Q}_{\frac{1}{2},\widetilde{\theta}_2}q), \tag{80b}$$

where $\mathbb{P}_{\theta_1,\theta_2}$, $\mathbb{Q}_{\widetilde{\theta}_1,\frac{1}{2}}$ and $\mathbb{Q}_{\frac{1}{2},\widetilde{\theta}_2}$ are the GGR projections defined in (46),(47) and (48) respectively.

In order to estimate ξ_u, we would like to set up the corresponding error equation. Owing to the smoothness assumption (43) of the exact solution, we can obtain the error equation

$$\langle e_{u,t}, v_h\rangle + B_h(\boldsymbol{e}, \boldsymbol{\chi}_h) = 0, \tag{81}$$

for any $\boldsymbol{\chi}_h = (v_h, r_h, s_h) \in \boldsymbol{V_h}$. Noticing the error decomposition (80) yields

$$\langle \xi_{u,t}, v_h\rangle + B_h(\boldsymbol{\xi}, \boldsymbol{\chi}_h) = \langle \eta_{u,t}, v_h\rangle + B_h(\boldsymbol{\eta}, \boldsymbol{\chi}_h) \equiv F_h^{\mathrm{err}}(t; \boldsymbol{\chi}_h) = \sum_{i=1}^{4} \mathcal{S}_i, \tag{82}$$

with

$$\begin{aligned}
\mathcal{S}_1 &= \langle (\eta_u)_t, v_h\rangle + \langle \eta_p, r_h\rangle + \langle \eta_q, s_h\rangle + \langle c\eta_u, v_h\rangle\,,\\
\mathcal{S}_2 &= \sqrt{\varepsilon}\mathcal{L}_1^{\widetilde{\theta}_1}(\eta_p, v_h) + \sqrt{\varepsilon}\mathcal{L}_2^{\widetilde{\theta}_2}(\eta_q, v_h),\\
\mathcal{S}_3 &= \sqrt{\varepsilon}\mathcal{K}_1^{\theta_1}(\eta_u, r_h) - \mathcal{H}_1(\eta_u, v_h),\\
\mathcal{S}_4 &= \sqrt{\varepsilon}\mathcal{K}_2^{\theta_2}(\eta_u, s_h) - \mathcal{H}_2(\eta_u, v_h).
\end{aligned}$$

Below we would like to estimate them separately. In this process, the GGR projections will play an important role.

(1) Estimate of $\mathcal{S}_1$. Using Cauchy-Schwarz inequality, we get directly that

$$\begin{aligned}
|\mathcal{S}_1| &\leq C\Big[\|\psi(\eta_u)_t\|^2 + \|\psi\eta_u\|^2 + \|\psi\eta_p\|^2 + \|\psi\eta_q\|^2\Big]^{\frac{1}{2}}\\
&\qquad\qquad \cdot \Big[\|\psi^{-1}v_h\|^2 + \|\psi^{-1}r_h\|^2 + \|\psi^{-1}s_h\|^2\Big]^{\frac{1}{2}}\\
&\leq C\Theta_1\|\boldsymbol{\chi}_h\|_\sharp,
\end{aligned}$$

where

$$\Theta_1 = \Big[\|\psi(\eta_u)_t\|^2 + \|\psi\eta_u\|^2 + \|\psi\eta_p\|^2 + \|\psi\eta_q\|^2\Big]^{\frac{1}{2}}. \tag{83}$$

(2) Estimate of $\mathcal{S}_2$. Taking into account the definitions of the projections $\mathbb{Q}_{\widetilde{\theta}_1,\frac{1}{2}}$ and $\mathbb{Q}_{\frac{1}{2},\widetilde{\theta}_2}$ in (47) and (48), we conclude that

$$\mathcal{S}_2 = -\sqrt{\varepsilon}\sum_{j=1}^{N_y}\int_{J_j}(\eta_p v_h)^-_{N_x+\frac{1}{2},y}\mathrm{d}y - \sqrt{\varepsilon}\sum_{i=1}^{N_x}\int_{I_i}(\eta_q v_h)^-_{x,N_y+\frac{1}{2}}\mathrm{d}x.$$

Using Cauchy-Schwarz inequality leads to

$$|\mathcal{S}_2| \leq C\sqrt{\varepsilon}\|\psi\eta_p\|_{\Gamma_h}\cdot \mathbb{J}_{x,\theta_1}(\psi^{-1}v_h) + C\sqrt{\varepsilon}\|\psi\eta_q\|_{\Gamma_h}\cdot \mathbb{J}_{y,\theta_2}(\psi^{-1}v_h) \leq C\Theta_2\|\boldsymbol{\chi}_h\|_\sharp,$$

where

$$\Theta_2 = \sqrt{\varepsilon}\Big[\|\psi\eta_p\|_{\Gamma_h} + \|\psi\eta_q\|_{\Gamma_h}\Big].$$

(3) Estimate of $\mathcal{S}_3$. Since the projection errors can not be eliminated completely, the superconvergence property of 2-d GGR projection has to be suitably exploited. To this end, we define

$$Z_{K_{ij}}(\eta_u, v_h) = \int_{K_{ij}}\eta_u(v_h)_x\mathrm{d}x\mathrm{d}y - \int_{J_j}\Big[(\eta_u^{\theta_1,y}v_h^-)_{i+\frac{1}{2},y} - (\eta_u^{\theta_1,y}v_h^+)_{i-\frac{1}{2},y}\Big]\mathrm{d}y, \tag{84}$$

on each element K_{ij}, where $\eta_u^{\theta_1,y} = \theta_1\eta_u^- + \widetilde{\theta}_1\eta_u^+$ at $(x_{i+\frac{1}{2}}, y)$ for $i = 0, 1, \cdots, N_x - 1$, and $(\eta_u^{\theta_1,y})_{N_x+\frac{1}{2},y} = (\eta_u^-)_{N_x+\frac{1}{2},y}$. Remark that $(\eta_u)^-_{\frac{1}{2},y}$ is understood as the projection error for the continuous extension function of u near the inflow boundary of Ω.

We can establish the following superconvergence property for the bilinear functional $Z_{K_{ij}}$.

Lemma 4.3. *Let the bilinear form $Z_{K_{ij}}(\eta_u, v_h)$ be defined in* (84). *For any $u \in H^{k+2}(\Omega)$, there exists a bounding constant C independent of σ, u and h such that*

$$\Big|\sum_{K_{ij}\in\Omega_h} Z_{K_{ij}}(\eta_u, v_h)\Big| \le Ch^{k+1}\big[|u|_{\psi,k+2} + \big(|\zeta_1|^\sigma + |\zeta_2|^\sigma\big)|u|_{k+2}\big]\|\psi^{-1}v_h\|, \tag{85}$$

holds for any $v_h \in V_h$, on the quasi-uniform Cartesian mesh, where $|\zeta_i| = |\widetilde{\theta}_i\theta_i^{-1}|$ for $i = 1, 2$, and ψ is the weight function defined in (15).

Proof. Following the proof line of identity (3.40) in Lemma 3.6 of [4], we can obtain

$$Z_{K_{ij}}(\eta_u, v_h) = 0, \qquad \forall u \in \mathcal{P}^{k+1}(\Omega_h), \quad \forall v_h \in V_h, \tag{86}$$

where $\mathcal{P}^{k+1}(\Omega_h)$ is made up of all piecewise polynomials of degree at most $k+1$ on each element in Ω_h.

Using Cauchy-Schwarz inequality, the inverse inequality (19) with weight function ψ^{-1}, and Lemma 4.2 with $s = 0$, we arrive at

$$\begin{aligned}\mathcal{LHS} \equiv \Big|\sum_{K_{ij}\in\Omega_h} Z_{K_{ij}}(\eta_u, v_h)\Big| &\le \|\psi\eta_u\|\|\psi^{-1}(v_h)_x\| + C\|\psi\eta_u\|_{\Gamma_h}\|\psi^{-1}v_h\|_{\Gamma_h}\\ &\le C\Big[h^{-1}\|\psi\eta_u\| + h^{-\frac{1}{2}}\|\psi\eta_u\|_{\Gamma_h}\Big]\|\psi^{-1}v_h\|\\ &\le C\Big[|u|_{\psi,1} + \big(|\zeta_1|^\sigma + |\zeta_2|^\sigma\big)|u|_1\Big]\|\psi^{-1}v_h\|.\end{aligned}$$

Therefore, using (86) we get that

$$\begin{aligned}\mathcal{LHS} &\le C \inf_{\chi\in\mathcal{P}^{k+1}(\Omega_h)}\Big\{|u-\chi|_{\psi,1} + \big(|\zeta_1|^\sigma + |\zeta_2|^\sigma\big)|u-\chi|_1\Big\}\|\psi^{-1}v_h\|\\ &\le Ch^{k+1}\Big[|u|_{\psi,k+2} + (|\zeta_1|^\sigma + |\zeta_2|^\sigma)|u|_{k+2}\Big]\|\psi^{-1}v_h\|,\end{aligned} \tag{87}$$

due to property (18). Hence we get the desired result of this lemma. ☐

Now we split $\mathcal{S}_3$ into two terms, namely, $\mathcal{S}_3 = \Lambda_1 + \Lambda_2$, where

$$\Lambda_1 = \sqrt{\varepsilon}\sum_{K_{ij}\in\Omega_h} Z_{K_{ij}}(\eta_u, r_h) - \beta_1\sum_{K_{ij}\in\Omega_h} Z_{K_{ij}}(\eta_u, v_h), \tag{88}$$

$$\begin{aligned}\Lambda_2 &= \sum_{j=1}^{N_y}\int_{J_j}\Big(\sqrt{\varepsilon}[\eta_u^- r_h^-]_{N_x+\frac{1}{2},y} - \sqrt{\varepsilon}[\eta_u^{\theta_1,y} r_h^+]_{\frac{1}{2},y}\\ &\qquad + \gamma_1[\eta_u^- v_h^-]_{N_x+\frac{1}{2},y} + \beta_1[\eta_u^{\theta_1,y} v_h^+]_{\frac{1}{2},y}\Big)\mathrm{d}y\\ &= \sum_{j=1}^{N_y}\int_{J_j}\Big(\sqrt{\varepsilon}[(g-\mathbb{P}_{\theta_2}^y g)r_h^-]_{N_x+\frac{1}{2},y} - \sqrt{\varepsilon}[(g-\mathbb{P}_{\theta_2}^y g)r_h^+]_{\frac{1}{2},y}\\ &\qquad + \gamma_1[(g-\mathbb{P}_{\theta_2}^y g)v_h^-]_{N_x+\frac{1}{2},y} + \beta_1[(g-\mathbb{P}_{\theta_2}^y g)v_h^+]_{\frac{1}{2},y}\Big)\mathrm{d}y.\end{aligned} \tag{89}$$

In the last step of (89), we have used the relationship (noting that $\theta_1 = 1$ when $i = N_x$)

$$(\mathbb{P}_{\theta_1,\theta_2}u)_{i+\frac{1}{2},y}^{\theta_1,y} = \mathbb{P}_{\theta_2}^y(u_{i+\frac{1}{2},y}^{\theta_1,y}), \quad \text{for } i = 0, 1, \cdots, N_x, \tag{90}$$

with $\mathbb{P}^y_{\theta_2}$ being 1-d GGR projection in y-direction which satisfies

$$\int_{J_j} (\mathbb{P}^y_{\theta_2} z) v_h \mathrm{d}y = \int_{J_j} z v_h \mathrm{d}y, \quad \forall v_h \in \mathcal{P}^{k-1}(J_j), \tag{91a}$$

$$(\mathbb{P}^y_{\theta_2} z)^{(\theta_2)}_{j+\frac{1}{2}} = z^{(\theta_2)}_{j+\frac{1}{2}}, \tag{91b}$$

for any $j = 1, 2, \ldots, N_y$, here $z^{(\theta_2)} = \theta_2 z^- + \widetilde{\theta}_2 z^+$, and $\theta_2 = 1$ when $j = N_y$.

We point out that the conclusion (90) can be easily verified according to the definition of GGR projection. Analogous treatment can also be found in [9]. For the completeness of this paper, we postpone the detailed proof in the Appendix.

By applying Lemma 4.3, we obtain

$$|\Lambda_1| \le C\Theta_3 \Big[\sqrt{\varepsilon}\|\psi^{-1} r_h\| + \beta_1 \|\psi^{-1} v_h\|\Big] \le C\Theta_3 \|\boldsymbol{\chi}_h\|_\sharp, \tag{92}$$

where

$$\Theta_3 = h^{k+1}\Big[|u|_{\psi,k+2} + (|\zeta_1|^\sigma + |\zeta_2|^\sigma)|u|_{k+2}\Big].$$

Using Cauchy-Schwarz inequality, inverse inequality (19) and $\varepsilon < h$ we get that

(93)

$$|\Lambda_2| \le C\|\psi(g - \mathbb{P}^y_{\theta_2} g)\|_{L^2(\Gamma_2)} \big[\sqrt{\varepsilon} h^{-\frac{1}{2}} \|\psi^{-1} r_h\| + \mathbb{J}_{x,\theta_1}(\psi^{-1} v_h)\big] \le C\Theta_4 \|\boldsymbol{\chi}_h\|_\sharp,$$

where Γ_2 is the collection of two vertical parts of boundary Γ, and

$$\Theta_4 = \|\psi(g - \mathbb{P}^y_{\theta_2} g)\|_{L^2(\Gamma_2)}.$$

Thus we obtain

$$|\mathcal{S}_3| \le C[\Theta_3 + \Theta_4]\|\boldsymbol{\chi}_h\|_\sharp. \tag{94}$$

(4) Estimate of $\mathcal{S}_4$. Following the similar argument as the estimate of $\mathcal{S}_3$, we can also obtain

$$|\mathcal{S}_4| \le C[\Theta_3 + \Theta_5]\|\boldsymbol{\chi}_h\|_\sharp. \tag{95}$$

where

$$\Theta_5 = \|\psi(g - \mathbb{P}^x_{\theta_1} g)\|_{L^2(\Gamma_1)},$$

where $\mathbb{P}^x_{\theta_1}$ is 1-d GGR projection in x-direction, which is similarly defined as $\mathbb{P}^y_{\theta_2}$, and Γ_1 is the collection of two horizontal parts of boundary Γ. We omit the details to save space.

Now we collect up the above estimates, and obtain from (82) that

$$\|F^{\mathrm{err}}_h(t)\|_\sharp = \sup_{\boldsymbol{\chi}_h \in \boldsymbol{V}_h} \frac{\sum_{i=1}^4 |\mathcal{S}_i|}{\|\boldsymbol{\chi}_h\|_\sharp} \le C \sum_{i=1}^5 \Theta_i. \tag{96}$$

So an application of Lemma 3.5 yields that

$$\|\psi \xi_u(T)\|^2 \le C\Big[\|\psi \xi_u(0)\|^2 + \int_0^T \sum_{i=1}^5 \Theta_i^2 \mathrm{d}t\Big]. \tag{97}$$

To obtain the optimal estimate, we need to adjust the parameters x_0, y_0 in the weight function and establish the following lemma.

Lemma 4.4. *Assume that $\varepsilon < h$ and σ is large enough. Let $x_0 = 1 - 2\mu_1\sigma h \log\frac{1}{h}$ and $y_0 = 1 - 2\mu_2\sigma h \log\frac{1}{h}$ with μ_1 and μ_2 large enough, then there holds*

$$\sum_{i=1}^{5} \Theta_i^2 \le Ch^{2k+2}, \quad \forall t \in [0,T], \tag{98}$$

where the bounding constant $C > 0$ is independent of σ,h and ε.

The proof is similar as Lemma 4.3 of [7], we put it in the Appendix. Now we come back to the local error estimate. By Lemma 4.4, we can obtain

$$\|\psi\eta_u(t)\| \le C\Theta_1 \le Ch^{k+1}, \quad t \in [0,T]. \tag{99}$$

Moreover, it follows from (97) that

$$\|\psi\xi_u(T)\|^2 \le C\|\psi\xi_u(0)\|^2 + Ch^{2k+2} \le Ch^{2k+2}, \tag{100}$$

due to the setting of the initial solution $\|\psi\xi_u(0)\| \le \|\psi(u_0 - \Pi_h u_0)\| + \|\psi\eta_u(0)\| \le Ch^{k+1}$ from the properties (20) and (99). Thus using the triangle inequality, we can derive the weighted L^2-norm error estimate $\|\psi e_u(T)\| \le Ch^{k+1}$ and the optimal error estimate

$$\|e_u(T)\|_{L^2(\Omega_0)} \le Ch^{k+1}, \tag{101}$$

in the local domain Ω_0, since the weight function is not smaller than one in Ω_0. This finishes the proof of Theorem 4.1.

5. Numerical experiments

In this section we present some numerical experiments to verify the convergence rates of the considered LDG scheme (6) with the GANF (7). For the spatial discretization, we adopt $\mathcal{Q}^1$ and $\mathcal{Q}^2$ elements on the nonuniform mesh, which is a 10% random perturbation the coordinates of horizontal lines and vertical lines of the uniform mesh, with the total number $N_x = N_y = N$. For the temporal discretization, we adopt the third order explicit total variation diminishing Runge-Kutta method [18]. The time step is taken as $\tau = 0.1h$ for piecewise linear polynomials, and $\tau = 0.05h$ for piecewise quadratic polynomials, respectively, where $h = 1/N$. The final computing time is set as $T = 0.1$.

We will verify the convergence rates in both the whole domain and the local region. To compute the local errors, we drop $\lfloor \log(1/h) \rfloor$ and $2\lfloor \log(1/h) \rfloor$ elements nearby the outflow boundaries for $\mathcal{Q}^1$ element and $\mathcal{Q}^2$ element, respectively. Here we have used the floor function $\lfloor r \rfloor$ to represent the greatest integer that is less than or equal to r. As for the GANF (7), four pairs of parameter $(\theta_1, \theta_2) = (0.8, 0.8), (1.0, 1.0), (0.8, 1.2), (1.2, 1.2)$ will be considered.

Example 1. We consider problem (1) with $\boldsymbol{\beta} = (1, 1)$, $\varepsilon = 10^{-5}$ and $c = 0$. Let the exact solution be

$$u(x, y, t) = e^{-t} \sin(\pi xy)(1 - e^{-\frac{1-x}{\varepsilon}})(1 - e^{-\frac{1-y}{\varepsilon}}). \tag{102}$$

The initial solution and the source term f can be determined by this solution. It is obvious that there are boundary layers along sides $x = 1$ and $y = 1$.

In Table 5 we list the L^2-norm errors and convergence orders in the whole domain and in the local region. From this table, we can observe the optimal convergence rate in a local domain, but not in the whole domain. This indicates the conclusion in Theorem 4.1 is sharp.

Example 2. In this example, we would like to investigate the error performance of the LDG method with the GANF for nonlinear SP problems. Let $\varepsilon = 10^{-5}$, consider

$$u_t + \left(\frac{u^2}{2}\right)_x + \left(\frac{u^2}{2}\right)_y - \varepsilon\Delta u = f, \tag{103}$$

with a suitably chosen f and initial solution such that the exact solution is the same as (102). In the design of the LDG method for solving the nonlinear problem (103), we define the numerical fluxes similarly as (7), namely, on the interior element interfaces

$$(\hat{h}_{1u}, \hat{h}_p)_{i+\frac{1}{2},y} = \begin{cases} (\frac{1}{2}(u_h^2)^{\theta_1,y} - \sqrt{\varepsilon}p_h^{\widetilde{\theta}_1,y}, -\sqrt{\varepsilon}u_h^{\theta_1,y})_{i+\frac{1}{2},y}, & \text{if } \min\{u_h^-, u_h^+\} > 0, \\ (\frac{1}{2}(u_h^2)^{\widetilde{\theta}_1,y} - \sqrt{\varepsilon}p_h^{\widetilde{\theta}_1,y}, -\sqrt{\varepsilon}u_h^{\theta_1,y})_{i+\frac{1}{2},y}, & \text{otherwise,} \end{cases} \tag{104}$$

for $i = 1, \cdots, N_x - 1$. And on Γ, we define

$$(\hat{h}_{1u}, \hat{h}_p)_{i+\frac{1}{2},y} = \begin{cases} (\frac{1}{2}g^2 - \sqrt{\varepsilon}p_h^+, -\sqrt{\varepsilon}g)_{\frac{1}{2},y}, & i = 0, \\ (\frac{1}{2}(u_h^-)^2 - \gamma_1(g - u_h^-) - \sqrt{\varepsilon}p_h^-, -\sqrt{\varepsilon}g)_{N_x+\frac{1}{2},y}, & i = N_x, \end{cases} \tag{105}$$

where g is the given Dirichlet boundary condition, the notations $\theta_1, \widetilde{\theta_1}, \gamma_1$ have the same meaning as before. We can also define the numerical flux $(\hat{h}_{2u}, \hat{h}_q)_{x,j+\frac{1}{2}}$ in a similar way, the details are omitted to save space.

The L^2-norm errors and convergence orders in the whole domain and local region are listed in Table 5. We can also observe the optimal local error accuracy, but see bad global error performance.

TABLE 1. L^2 errors and orders of accuracy on nonuniform mesh for Example 1.

			$(\theta_1, \theta_2) = (0.8, 0.8)$		$(\theta_1, \theta_2) = (1.0, 1.0)$		$(\theta_1, \theta_2) = (0.8, 1.2)$		$(\theta_1, \theta_2) = (1.2, 1.2)$	
		N	L^2-error	order	L^2-error	order	L^2-error	order	L^2-error	order
Global	$\mathcal{Q}^1$	32	4.14E-02	-	4.14E-02	-	4.14E-02	-	4.14E-02	-
		64	3.00E-02	0.46	3.00E-02	0.46	3.00E-02	0.46	3.00E-02	0.46
		128	2.09E-02	0.53	2.09E-02	0.53	2.09E-02	0.53	2.09E-02	0.53
		256	1.53E-02	0.44	1.53E-02	0.44	1.53E-02	0.44	1.53E-02	0.44
		512	1.07E-02	0.52	1.07E-02	0.52	1.07E-02	0.52	1.07E-02	0.52
	$\mathcal{Q}^2$	32	4.13E-02	-	4.13E-02	-	4.13E-02	-	4.13E-02	-
		64	2.99E-02	0.47	2.99E-02	0.47	2.99E-02	0.47	2.99E-02	0.47
		128	2.07E-02	0.53	2.07E-02	0.53	2.07E-02	0.53	2.07E-02	0.53
		256	1.51E-02	0.45	1.51E-02	0.45	1.51E-02	0.45	1.51E-02	0.45
		512	1.04E-02	0.54	1.04E-02	0.54	1.04E-02	0.54	1.04E-02	0.54
Local	$\mathcal{Q}^1$	32	3.04E-04	-	2.14E-04	-	2.46E-04	-	1.82E-04	-
		64	8.51E-05	1.84	5.99E-05	1.84	6.87E-05	1.84	5.09E-05	1.83
		128	2.33E-05	1.87	1.65E-05	1.86	1.89E-05	1.86	1.41E-05	1.86
		256	6.04E-06	1.95	4.25E-06	1.95	4.87E-06	1.95	3.61E-06	1.96
		512	1.55E-06	1.96	1.09E-06	1.96	1.25E-06	1.96	9.29E-07	1.96
	$\mathcal{Q}^2$	32	6.97E-07	-	8.29E-07	-	8.83E-07	-	9.93E-07	-
		64	1.14E-07	2.61	1.35E-07	2.61	1.44E-07	2.61	1.63E-07	2.61
		128	1.98E-08	2.53	2.22E-08	2.61	2.41E-08	2.58	2.69E-08	2.60
		256	2.67E-09	2.89	3.11E-09	2.84	3.35E-09	2.85	3.77E-09	2.84
		512	3.56E-10	2.91	4.20E-10	2.89	4.50E-10	2.90	5.09E-10	2.89

6. Concluding remarks

In this paper, we present the local stability and local error estimates of the LDG scheme with the generalized alternating numerical flux, for the two-dimensional singularly perturbed problems with outflow boundary layers. Double-optimal error estimate is obtained for the piecewise tensor product polynomials on quasi-uniform Cartesian meshes. The technical difficulty lies in establishing the optimal

TABLE 2. L^2 errors and orders of accuracy on nonuniform mesh for Example 2.

			$(\theta_1,\theta_2)=(0.8,0.8)$		$(\theta_1,\theta_2)=(1.0,1.0)$		$(\theta_1,\theta_2)=(0.8,1.2)$		$(\theta_1,\theta_2)=(1.2,1.2)$	
		N	L^2-error	order	L^2-error	order	L^2-error	order	L^2-error	order
Global	$\mathcal{Q}^1$	32	4.14E-02	-	4.14E-02	-	4.14E-02	-	4.14E-02	-
		64	3.00E-02	0.46	3.00E-02	0.46	3.00E-02	0.46	3.00E-02	0.46
		128	2.08E-02	0.53	2.08E-02	0.53	2.08E-02	0.53	2.08E-02	0.53
		256	1.52E-02	0.45	1.52E-02	0.45	1.52E-02	0.45	1.52E-02	0.45
		512	1.06E-02	0.52	1.06E-02	0.52	1.06E-02	0.52	1.06E-02	0.52
	$\mathcal{Q}^2$	32	4.13E-02	-	4.13E-02	-	4.13E-02	-	4.13E-02	-
		64	2.98E-02	0.47	2.98E-02	0.47	2.98E-02	0.47	2.98E-02	0.47
		128	2.06E-02	0.53	2.06E-02	0.53	2.06E-02	0.53	2.06E-02	0.53
		256	1.50E-02	0.46	1.50E-02	0.46	1.50E-02	0.46	1.50E-02	0.46
		512	1.02E-02	0.55	1.02E-02	0.55	1.02E-02	0.55	1.02E-02	0.55
Local	$\mathcal{Q}^1$	32	3.06E-04	-	2.15E-04	-	2.47E-04	-	1.82E-04	-
		64	8.54E-05	1.84	6.00E-05	1.84	6.89E-05	1.84	5.10E-05	1.83
		128	2.34E-05	1.87	1.65E-05	1.86	1.89E-05	1.86	1.41E-05	1.85
		256	6.05E-06	1.95	4.25E-06	1.95	4.88E-06	1.96	3.62E-06	1.96
		512	1.55E-06	1.96	1.09E-06	1.97	1.25E-06	1.96	9.30E-07	1.96
	$\mathcal{Q}^2$	32	7.15E-07	-	8.58E-07	-	9.14E-07	-	1.03E-06	-
		64	1.16E-07	2.62	1.39E-07	2.63	1.48E-07	2.62	1.68E-07	2.62
		128	2.08E-08	2.48	2.26E-08	2.62	2.48E-08	2.58	2.74E-08	2.62
		256	2.72E-09	2.94	3.14E-09	2.85	3.40E-09	2.87	3.81E-09	2.85
		512	3.58E-10	2.93	4.21E-10	2.90	4.53E-10	2.91	5.11E-10	2.90

approximation property and superconvergence property for the two-dimensional G-GR projection equipped with the weight function. In the future, we will consider the LDG method for the singularly perturbed problem with other type layers, such as parabolic boundary layer, interior layer or corner singularities.

Appendix

In this Appendix, we supplement some technical proofs.

Proof of Lemma 4.4. Using Lemma 4.2 of [7], we can obtain that

$$\Theta_4 \le Ch^{k+1}\Big[\|\psi D_y^{k+1} g\|_{L^2(\Gamma_2)} + |\zeta_2|^\sigma \|D_y^{k+1} g\|_{L^2(\Gamma_2)}\Big], \tag{A.1}$$

$$\Theta_5 \le Ch^{k+1}\Big[\|\psi D_x^{k+1} g\|_{L^2(\Gamma_1)} + |\zeta_1|^\sigma \|D_x^{k+1} g\|_{L^2(\Gamma_1)}\Big]. \tag{A.2}$$

Due to Lemma 4.2 and $\varepsilon < h$, it is sufficient to prove that

$$|z|_{\psi,k+1} \le C, \quad \zeta^\sigma |z|_{k+1} \le C, \quad \text{for} \quad z = u, p, q, u_t, u_x, u_y, g, \tag{A.3}$$

where $\zeta \equiv \max\{|\zeta_1|, |\zeta_2|\}$.

To this end, we take $z = u$ as an example, since the remaining cases can be proved in the similar way. Let $\widetilde{\Omega}_0 = (0, \widetilde{x}_0) \times (0, \widetilde{y}_0)$ with $\widetilde{x}_0 = 1 - \mu_1 \sigma h \log \frac{1}{h}$ and $\widetilde{y}_0 = 1 - \mu_2 \sigma h \log \frac{1}{h}$, such that

$$\Omega_{\text{local}} = \bigcup_{K_{ij}\cap\widetilde{\Omega}_0 \neq \emptyset} \overline{K}_{ij} \subseteq \Omega_{\text{sm}} = \Big(0, 1 - \rho_1 \varepsilon \log \frac{1}{\varepsilon}\Big) \times \Big(0, 1 - \rho_2 \varepsilon \log \frac{1}{\varepsilon}\Big). \tag{A.4}$$

This can be done if $\mu_i \sigma \ge 2\rho_i$ $(i = 1, 2)$, since $\varepsilon < h$. Assume that there exist two constants h_0 and m_0 such that $h_0^{m_0} \le \varepsilon \le h \le h_0 < 1$, then it follows from the smoothness assumption (44) and the boundedness property of weight function that

$$\begin{aligned}
|z|_{\psi,k+1}^2 &= \sum_{i+j=k+1} \|\psi D_x^i D_y^j z\|^2 \\
&\le C \sum_{i+j=k+1} \|D_x^i D_y^j z\|^2_{L^2(\Omega_{\text{local}})} + Ch^{2\mu} \sum_{i+j=k+1} \|D_x^i D_y^j z\|^2_{L^2(\Omega\setminus\Omega_{\text{local}})} \\
&\le C + Ch^{2\mu}\varepsilon^{-2(k+1)} \le C + Ch_0^{2\mu-2(k+1)m_0} \le C,
\end{aligned} \tag{A.5}$$

if $\mu \geq (k+1)m_0$. Furthermore, it is easy to see that $\zeta^\sigma |z|_{k+1} = 0$ when $\zeta = 0$. Otherwise, if $\zeta \neq 0$, we also have

(A.6)
$$\zeta^{2\sigma}|z|_{k+1}^2 = \zeta^{2\sigma} \sum_{i+j=k+1} \|D_x^i D_y^j z\|^2 \leq C\zeta^{2\sigma}\varepsilon^{-2(k+1)} \leq C\zeta^{2\sigma}h_0^{-2(k+1)m_0} \leq C,$$

by taking σ large enough, for example, $\sigma \geq (k+1)m_0 \log h_0/\log\zeta$. Hence Lemma 4.4 is proved. □

Proof of (90)**.** Owing to the definition of GGR projection $\mathbb{P}_{\theta_1,\theta_2}$ and the definition of the weighted averages, we have

$$\text{(A.7)} \quad \int_{J_j} (\mathbb{P}_{\theta_1,\theta_2}u)_{i+\frac{1}{2},y}^{\theta_1,y} v_h(y)\mathrm{d}y = \int_{J_j} u_{i+\frac{1}{2},y}^{\theta_1,y} v_h(y)\mathrm{d}y, \quad \forall v_h(y) \in \mathcal{P}^{k-1}(J_j),$$

$$\begin{aligned} \left[(\mathbb{P}_{\theta_1,\theta_2}u)_{i+\frac{1}{2},y}^{\theta_1,y}\right]_{j+\frac{1}{2}}^{(\theta_2)} &= (\mathbb{P}_{\theta_1,\theta_2}u)_{i+\frac{1}{2},j+\frac{1}{2}}^{\theta_1,\theta_2} \\ &= u_{i+\frac{1}{2},j+\frac{1}{2}}^{\theta_1,\theta_2} = \left[u_{i+\frac{1}{2},y}^{\theta_1,y}\right]_{j+\frac{1}{2}}^{(\theta_2)}, \quad j = 1,2,\ldots,N_y, \end{aligned} \quad \text{(A.8)}$$

for any $i = 0,1,2,\ldots,N_x$. This shows that $(\mathbb{P}_{\theta_1,\theta_2}u)_{i+\frac{1}{2},y}^{\theta_1,y}$ satisfies the same conditions as the 1-d GGR projection $\mathbb{P}_{\theta_2}^y(u_{i+\frac{1}{2},y}^{\theta_1,y})$. Since both of them are polynomials of degree at most k for the variable y, due to the unique existence of 1-d GGR projection $\mathbb{P}_{\theta_2}^y$ (see Lemma 4.1 of [7]), we conclude that they are equal. □

Acknowledgments

This research was supported by NSFC grants 11671199, 11601241 and 11571290, Natural Science Foundation of Jiangsu Province grants BK20160877 and BK20170374, Nature Science Research Program for Colleges and Universities of Jiangsu Province grant 17KJB110016, SUST grant 331712102 and NUPTSF grant NY215067.

References

[1] F. Bassi, S. Rebay, A high-order accurate discontinuous finite element method for the numerical solution of the compressible Navier-Stokes equations, J. Comput. Phys., 131 (1997), pp. 267–279.

[2] E. Burman, J. Guzmán and D. Leykekhman, Weighted error estimates of the continuous interior penalty method for singularly perturbed problems, IMA J. Numer. Anal., 29 (2009), pp. 284–314.

[3] P. Castillo, B. Cockburn, D. Schötzau and C. Schwab, Optimal a priori error estimates for the hp-version of the local discontinuous Galerkin method for convection-diffusion problems, Math. Comp., 71 (2001), pp. 455–478.

[4] Y. Cheng, X. Meng, and Q. Zhang, Application of generalized Gauss–Radau projections for the local discontinuous Galerkin method for linear convection-diffusion equations, Math. Comp., 86 (2017), pp. 1233–1267.

[5] Y. Cheng, F. Zhang, and Q. Zhang, Local analysis of local discontinuous Galerkin method for the time-dependent singularly perturbed problem, J. Sci. Comput., 63 (2015), pp. 452–477.

[6] Y. Cheng and Q. Zhang, Local analysis of the fully discrete local discontinuous Galerkin method for the time-dependent singularly perturbed problem, J. Comput. Math., 35:3 (2017), pp. 265-288.

[7] Y. Cheng and Q. Zhang, Local analysis of the local discontinuous Galerkin method with generalized alternating numerical flux for one-dimensional singularly perturbed problem, J. Sci. Comput., 72 (2017), pp. 792-819.

[8] B. Cockburn and C.-W. Shu, The local discontinuous Galerkin method for time-dependent convection-diffusion systems, SIAM J. Numer. Anal., 35 (1998), pp. 2440–2463.

[9] B. Cockburn, G. Kanschat, I. Perugia and D. Schötzau, Superconvergence of the local discontinuous Galerkin method for elliptic problems on Cartesian grids, SIAM J. Numer. Anal., 39:1 (2001), pp. 264–285.

[10] J. Guzmán, Local analysis of discontinuous Galerkin methods applied to singularly perturbed problems, J. Numer. Math., 14:1 (2006), pp. 41–56.
[11] J. S. Hesthaven and T. Warburton, Nodal Discontinuous Galerkin Methods: Algorithms, Analysis, and Applications, Springer, New York, 2008.
[12] R. A. Horn and C. R. Johnson, Topic in Matix Analysis, Cambridge Univeristy Press, Cambridge, 1991.
[13] C. Johnson, U. Nävert and J. Pitkäranta, Finite element methods for linear hyperbolic problems, Comput. Methods Appl. Mech. Engrg., 45 (1984), pp. 285–312.
[14] C. Johnson, A. Schatz and L. Wahlbin, Crosswind swear and pointwise errors in the streamline diffusion finite element methods, Math. Comp., 49:179 (1987), pp. 25–38.
[15] H. Liu and N. Ploymaklam, A local discontinuous Galerkin method for the Burgers-Poisson equation, Numer. Math., 129 (2015), pp. 321–351.
[16] X. Meng, C.-W. Shu, and B. Wu, Optimal error estimates for discontinuous Galerkin methods based on upwind-biased fluxes for linear hyperbolic equations, Math. Comp., 85:299 (2016), pp. 1225–1261.
[17] H. G. Roos, M. Stynes, and L. Tobiska, Robust Numerical Methods for Singularly Perturbed Differential Equations, Springer, Berlin, 2008.
[18] C.-W. Shu and S. Osher, Efficient implementation of essentially non-oscillatory shock capturing schemes, J. Comput. Phys., 77 (1988), pp. 439–471.
[19] H. J. Wang and Q. Zhang, Error estimate on a fully discrete local discontinuous Galerkin method for linear convection-diffusion problem, J. Comput. Math., 31:3(2013), pp. 283–307.
[20] M. Vlasak and H.-G. Roos, An optimal uniform a priori error estimate for an unsteady singularly perturbed problem, Int. J. Numer. Anal. Mod., 11:1 (2014), pp. 24–33.
[21] Y. Xu and C.-W. Shu, Local discontinous Galerkin methods for high-order time-dependent partial differetial equations, Commun. Comput. Phys., 7 (2010), pp. 1–46.
[22] Q. Zhang and C.-W. Shu, Error estimates for the third order explicit Runge-Kutta discontinuous Galerkin method for a linear hyperbolic equation in one-dimension with discontinuous initial data, Numer. Math., 126:4 (2014), pp. 703–740.
[23] H. Q. Zhu and Z. M. Zhang, Local error estimates of the LDG method for 1-D singularly perturbed problems, Int. J. Numer. Anal. Mod., 10:2 (2013), pp. 350–373.

School of Mathematics and Physics, Suzhou University of Science and Technology, Suzhou 215009, China.
E-mail: ycheng@usts.edu.cn.

Department of Mathematics, Nanjing University, Nanjing 210093, China.
E-mail: qzh@nju.edu.cn

College of Science, Nanjing University of Posts and Telecommunications, Nanjing 210023, China.
E-mail: hjwang@njupt.edu.cn